ROYAL SOCIETY
OF CHEMISTRY

Check for updates

Microfluidics for antibiotic susceptibility testing

Witold Postek, [ID] *[ab] Natalia Pacocha[a] and Piotr Garstecki [ID] *[a]

The rise of antibiotic resistance is a threat to global health. Rapid and comprehensive analysis of infectious strains is critical to reducing the global use of antibiotics, as informed antibiotic use could slow down the emergence of resistant strains worldwide. Multiple platforms for antibiotic susceptibility testing (AST) have been developed with the use of microfluidic solutions. Here we describe microfluidic systems that have been proposed to aid AST. We identify the key contributions in overcoming outstanding challenges associated with the required degree of multiplexing, reduction of detection time, scalability, ease of use, and capacity for commercialization. We introduce the reader to microfluidics in general, and we analyze the challenges and opportunities related to the field of microfluidic AST.

1. Antibiotic resistance crisis

Once called 'miracle drugs', antibiotics help humanity keep infectious diseases at bay. Since the dawn of antibiotics, strains of bacteria resistant to antibiotic effects have been reported – Alexander Fleming, famous for discovering the effect of penicillin on bacteria, mentioned the irresponsible use of antibiotics and the threat of drug-resistant bacteria as early as 1945 in his Nobel Lecture.[1] The number of new antibiotics introduced to the clinic decreases over time, while the number of resistant strains increases.[2] Antibiotic-resistant infections are responsible for *ca.* 33 000 deaths per year in the European Union[3] and around 35 000 deaths per year in the USA,[4] with the most deadly infection in the USA being caused by *Clostridioides difficile*, methicillin-resistant *Staphylococcus aureus* (MRSA), and extended-spectrum beta-lactamase (ESBL) producing *Escherichia coli.*[4] Although most deaths caused by bacterial agents could be treated with antibiotics,[5] the number of fatalities caused by antibiotic resistant bacteria is predicted to increase to a stagerring 10 million death per year in 2050 as predicted by WHO.[5] This prediction is sometimes criticized,[6] but even these critics agree that the antibiotic resistance of bacteria is a major health challenge now and in the predictable future. A wide-scale statistical analysis based on Global Burden of Disease Study,[7] showed that the 2016 estimate of 700 000 deaths[8,9] per year by antibiotic resistant bacteria might be too shy: research showed that 1.27 million deaths per year can be directly attributed to antibiotic-resistant bacteria (if all antibiotic-resistant infections were replaced by no infection, 4.95 million deaths would have been

avoided in 2019, while if all antibiotic-resistant infections were replaced by antibiotic-susceptible infections, 1.27 million deaths could have been prevented[8]). The data from the statistical analysis inform that it is not only the lack of sanitation or access to antibiotics that drive bacteria-related deaths, as antibiotic resistance plays a large role there. The geographic distribution of deaths *per capita* attributable to antibiotic resistant bacteria shows an expected tilt towards low-to-medium income countries, but the difference in *per capita* deaths by antibiotic resistant microbes between those and high income countries is not huge: antibiotic resistant bacteria are causing death and suffering worldwide.[8]

Bacteria resistant to multiple drugs at once, or even to all clinically available antibiotics, are of serious concern to researchers.[10,11] It is estimated that more than 50% of antibiotics prescribed[2,12] around the world is used either unnecessarily (*e.g.*, for viral infections) or wrongly (either wrong narrow-spectrum antibiotic or blindly used broad-spectrum antibiotic that leads to intense growth of antibiotic-resistant strains that are usually kept in check by the rest of microbiota of a healthy human).[13] Antibiotic resistance is also emerging due to antibiotic pollution in the environment,[14] which suggests that combating antibiotic resistance should involve collaboration of multiple sectors, such as public health, animal health, plant health – as specified in the WHO's One Health approach.[15] To curb the emergence of antibiotic resistance, it is imperative to reduce the overuse of antibiotics. We need more cheap and easy-to-use platforms for the identification of pathogens and for assessment of antibiotic resistance to stop the inappropriate use of antibiotics and perhaps limit the incorrect use of antibiotics – physicians with access to a point-of-care platform for identification of pathogens and their resistance are less likely to prescribe antibiotics when they are not needed.[16–18] As a prolonged diagnosis of a pathogen and its

[a] *Institute of Physical Chemistry of the Polish Academy of Sciences, ul. Kasprzaka 44/52, 01-224 Warszawa, Poland. E-mail: pgarstecki@ichf.edu.pl*
[b] *Broad Institute of MIT and Harvard, Merkin Building, 415 Main St, Cambridge, MA 02142, USA. E-mail: wpostek@broadinstitute.org*

antibiotic resistance profile decreases the chance of survival of an infected patient, the time from sampling to diagnosis should be reduced to a minimum. Therefore any new platform that could be used to diagnose bacterial infections should be as rapid as possible.

Quantitatively, bacterial drug resistance is established by measuring a parameter called minimum inhibitory concentration (MIC), the lowest concentration of a drug that prevents the growth of bacteria.[19] MIC measurements are the basis for establishing resistance breakpoints by agencies such as CLSI or EUCAST.[20] A breakpoint is a drug concentration against which a patient sample is tested – if there is growth, the bacterial strain is resistant; if there is no growth, the strain is susceptible. Setting breakpoint values by medical agencies is based on MIC and pharmacokinetics and pharmacodynamics (PK/PD) of an antibiotic.[21] Clinicians use breakpoint values based on the MIC, but not the MIC itself. Breakpoint values, although highly useful, do not convey the information that an MIC screen personalized to a given patient would: *e.g.*, a breakpoint does not necessarily take into account a wild-type resistance distribution, which can lead to both false positives and false negatives, or there is a possibility that a tested bacterium does have a resistance mechanism but is still below the breakpoint.[22]

The gold standard assays for establishing MIC are broth dilution and e-test. The most commonly used automated platform for quantifying MIC is VITEK® 2 by bioMérieux, based on the microbroth dilution method. VITEK® 2 uses cassettes with a set of compartments with a diluted drug and with the tested bacteria. The compartments are monitored constantly to generate a growth curve which is compared to a growth curve of bacteria with a known reference MIC. All the upcoming automated AST solutions have to be compared to this or similar devices (*e.g.*, BD Phoenix by BD Diagnostics, Sensititre by Thermo Scientific, MicroScan by Siemens HC Diagnostics) as a standard if they are to be used in a clinical setting on a wide scale. A potent source of innovation in the area of automated broth dilution is microfluidics, and this is visible in various emerging start-up companies that try and develop disruptive technologies for AST.

Due to poor profit prospects on new antibiotics, big pharmaceutical companies are not inclined to spend money on antibiotic research and clinical trials.[23] To tackle the growing levels of antimicrobial resistance, governments and international bodies are implementing push and pull strategies to incentivize the development of new antibiotics by private companies.[24–26] Push strategies include direct grants and tax incentives, while pull strategies consist of milestone rewards or market exclusivity extensions.[23] As an example of a pull strategy, the Longitude Prize of £10 million was set for a competitor that develops a point-of-care diagnostic test that will help conserve the usage of antibiotics. A few essential criteria are required to be considered for the prize: the test must be needed, accurate, affordable, rapid, easy to use, safe, and scalable. These requirements, relatively easy to achieve in separation, pose a

significant technical challenge when combined. In recent years, there has been a surge of scientific publications about point-of-care, rapid, easy-to-use platforms for a number of biological applications. A considerable proportion of the presented solutions is based on microfluidics and tackle the antibiotic resistance problem.

In this review, we comprehensively describe many of the microfluidic systems that were applied to quantitative antibiotic resistance assessment. There is a need for quantitative antibiotic susceptibility testing systems[27] as they provide more information than just the detection of resistance or susceptibility, and we identify assay multiplexing and signal detection time as the bottlenecks to the development of rapid AST with an MIC output. We therefore focus on the microfluidic technologies applied to AST to inform the reader which technology suits different multiplexing or detection methods. We put the most effort here to describe microfluidic solutions that not only identify antibiotic resistance, but also generate the MIC which we consider highly informative in medical diagnostics. We recommend that the reader reaches for other review articles that describe in detail different aspects of microfluidics applied to antibiotic susceptibility screens or are related to AST, such as strictly single-cell assays,[28] technical challenges to manufacturing AST devices at scale,[29] microfluidics put in a broader AST context,[27,30,31] or barriers to the development of rapid AST platforms.[32] For a recent list of innovative companies in the field of AST we send the reader elsewhere.[27] We begin with a description of microfluidic systems in general that will allow the reader to understand how microfluidic systems for biological applications work and where to seek technical improvements. We divide the microfluidic platforms for AST into categories by the approach to liquid handling (Fig. 1), as this determines the assay's capabilities and challenges in the assay's potential development: static chamber arrays, flow chamber arrays, droplet arrays, and systems based on flowing droplets. A separate category is the systems for phenotypic-molecular ("pheno-molecular") assessment of MIC in microfluidics. Among all the microfluidic platforms we describe, we highlight platforms that allow for single-cell level studies, as these platforms allow for either rapid AST or heterogeneity studies. We conclude this review with a discussion on the challenges that researchers face when working on microfluidic platforms for analysis of antibiotic resistance, and with identification of research opportunities in application of microfluidic techniques to AST.

2. Microfluidic methods of studying bacteria

2.1. Introduction

Microfluidics is now a matured field of science that deals with the flows of fluids at microscopic scales. The flows are realized mainly within the confinement of microchannels that tend to have hydraulic diameters in the range of tens to
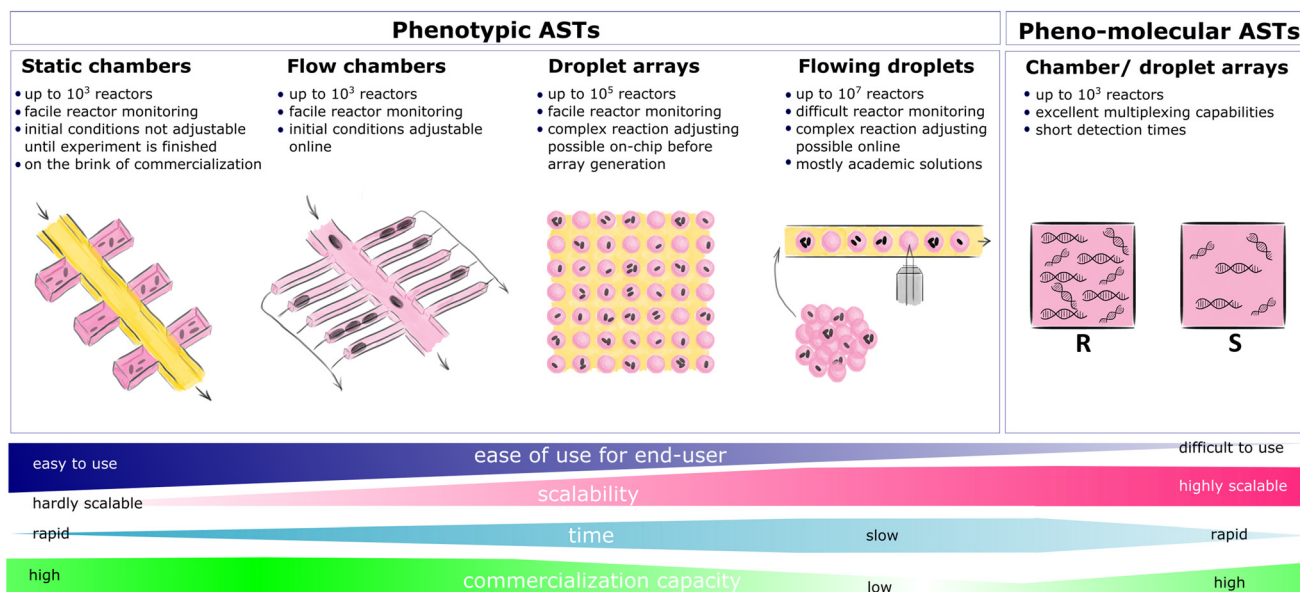
Fig. 1 Schematic representation of microfluidic approaches used in antibiotic susceptibility testing. A given microfluidic solution is easier to use for an end-user at the cost of the process scale and the flexibility of the assay, *i.e.*, multiplexing capabilities or on-chip operations. Static microfluidic chambers are, in principle, an array of wells in a well plate with automated filling and separating operations added. Static chambers provide for some multiplexing: antibiotics in different concentrations can be printed to separate chambers, and the monitoring of cells is easy as the chambers are not numerous and they do not move, so the cells are immobile for the sake of microscopy. Static chambers are feasible for transfer to commercial applications as they are easy to produce at scale. Flow chambers are similar to static chambers, albeit their content can be gradually changed over the course of an experiment, usually through diffusion from the main channel to the side chambers. Hybrid droplet arrays offer greater scale and multiplexing than chambers, and they still allow for easy monitoring of cells, as the droplets are immobile. Complex operations on liquids can be done on-chip before generation and immobilization of droplets. However, after immobilizing the droplets, it is difficult to introduce changes to reaction conditions controllably for each droplet. The use of droplets requires consideration of the transport of matter, *e.g.*, antibiotics or dyes, between droplets, although in stationary arrays the droplets are not moving, so the surfactant-based transfer of molecules should be limited. Flowing droplets provide superb scale and multiplexing capabilities, as complex liquid handling operations can be done even at the level of single droplets. Droplets are usually incubated for the growth of encapsulated bacteria for long times, so the transfer of matter between droplets must be considered. Monitoring of cell growth dynamics is not trivial, as droplets move during incubation due to mixing or convection, so following the same droplet over the course of the experiment would pose a considerable challenge. Flowing droplet arrays are complex to automate from end to end; therefore, they are not easily transferable to commercial settings. However, flowing droplet arrays provide for vast research possibilities due to the scale of possible experiments. Pheno-molecular ASTs are different in that they can in principle be performed in droplets or static chambers. Although the currently used number of reactors for pheno-molecular assays is smaller than in droplet-based assays, this approach has great potential due to short sample-to-result time and high multiplexing capabilities.

hundreds of micrometers – such small diameters guarantee the laminar flow regime inside the channels, implications of which we discuss below. The flows are generated either by positive pressure – syringe pumps and compressed air systems – or negative pressure – vacuum pumps. Channels are usually made with soft lithography[33] or CNC milling,[34] and the resulting microfluidic devices, or chips, are made of elastomers (most notably polydimethylsiloxane, PDMS[35,36]), glass, thermoplastics, or hybrids of these materials. PDMS is often used for devices housing living organisms as this polymer is permeable to gases, thus granting good oxidation of the contained cells. Numerous review articles are available detailing the technical side of the microfluidic chip, covering fabrication of devices,[37] generation of droplets,[38] and physics of flow.[39] Microfluidic systems are broadly divided into the ones that contain only one liquid phase (single-phase microfluidics) or two and more phases.

2.1.1. Single-phase microfluidics. The flow of liquids in microchannels is realized almost exclusively in the laminar

regime, where the layers of flowing fluids do not intermingle as in the case of turbulent flows. This means that mixing in microchannels happens through diffusion between liquid layers (which practically means that the mixing is slow) and that the flow can be precisely controlled, which led to such early developments as the microfluidic linear concentration gradient generator.[40] The field has also benefitted from the integration of microvalves into chips.[41] The most significant advantage of single-phase systems over droplet-based microfluidics in microbiology is the potential to immobilize cultured organisms that allows for precise optical measurements.[42] The volume of the chambers within the single-phase microfluidic systems is confined between several hundred picoliters and single milliliters. Achieving smaller chamber volumes is difficult due to technical issues of manufacturing and later controlling liquid flows in extremely small channels. The control of chamber content during experiments is difficult due to diffusion issues and the fact that the chambers are practically separated from the main channel.

When a sample is partitioned into chambers and separated by *e.g.* oil it is possible to replace the oil with the aqueous phase to introduce new compounds into chambers. This procedure might be daunting as chambers are usually explicitly designed so that there is no diffusion of particles between chambers during experiments, *e.g.* chambers are connected with the main device channel with narrow and long connector channels. This chamber content control issue results in assays that are either locked with a specific set of reagents from the beginning to the end of the experiment[43] (static chambers) or in assays in which the content changes gradually through diffusion from the main channel[44] (flow chambers).

2.1.2. Droplets and multi-phase microfluidics. Multiphase microfluidics deals with the flow of segmented fluids, such as air bubbles in water or water droplets submerged in oil.[45,46] Droplets within microchannels can be precisely moved, split, joined, or immobilized. It is possible to form monodisperse emulsions of attoliter-sized droplets,[47] although droplets of sizes in the range of picoliters to nanoliters are more practical. The most popular production method of emulsions in microfluidics is flow-focusing,[48] with a single module capable of generating droplets with a frequency in the range of several kilohertz (kHz), recently up-scaled and parallelized into a system that generated droplets at *ca.* 8 MHz.[49] In this context, the detection of signals from droplets generated this frequent is a bottleneck, as only recently state-of-the-art technology was shown to detect signals from droplets at frequency of 1 MHz.[50] Similar frequencies of generation of droplets are achievable by parallelization of step emulsification modules.[51] Step emulsification is a mechanism of droplet generation that requires less equipment than flow-focusing and is easy to parallelize, albeit a single step-emulsification module generates droplets orders of magnitude slower than a single flow-focusing module. Implementing droplet-based systems to a laboratory does not require complicated setups known from microfluidics-centered laboratories that usually consist of syringe pumps/pressure controllers to generate the flow of liquids, tubing connecting syringes to a microfluidic chip placed on a custom-made camera setup. Successful research on cells was performed with systems using droplets generated by user-friendly Biorad QX200 device[52,53] designed for droplet digital PCR, droplets generated by vortexing a sample with submerged beads,[54] or droplets generated passively by gravity.[55] To house biological reactions in droplets, it is imperative to use biocompatible materials and liquids: as the cells usually thrive in an aqueous environment, the droplets also have to be aqueous. To sustain living organisms inside droplets, these droplets should be submerged in oil with high oxygen solubility, so fluorinated oils are usually employed. To prevent unwanted coalescence of droplets, their surfaces should be coated with biocompatible surfactants,[56,57] and to avoid wetting the channel walls by droplets, chemical modification of microchannel walls with fluorinated compounds should be done.[58] It is possible to encapsulate single objects, *e.g.*, cells,

in separate droplets. This is done by diluting a cell solution so that the number of cells in a solution is significantly smaller than the number of droplets generated from this solution – this method is called stochastic confinement,[59] and has been applied successfully to a PCR variation called digital PCR[60] or in single-cell level genomics.[61–63]

A separate branch of multiphase microfluidic devices contains lab-on-a-disc systems, *i.e.*, discus-shaped microfluidic devices with embedded channels specially engineered so that when the disc is spun on a centrifuge, the samples move sequentially between the chambers on the disc. The sequential release of liquids is based on capillary valves designed to break when a specific centrifugal force is reached in the device. We encourage the reader to find a detailed description of centrifugal microfluidic devices and recent developments in biomedical research in lab-on-a-disc devices elsewhere.[64,65] Although not trivial to engineer, lab-on-a-disc diagnostic devices have great commercialization potential due to the ease of use for the end-user when the device is assembled.

2.2. Microfluidic static chambers for quantitative AST

2.2.1. Population-level studies in microfluidic static chambers. One of the earliest examples of microfluidic chambers for AST is from 2010 (ref. 66) when the authors used separate microfluidic channels to house bacteria growing in the presence of antibiotics. This approach required pipetting every antibiotic concentration to a separate channel, which is impractical when considering large-scale screening experiments. Still, the authors demonstrated beneficial data for microbiology in microfluidics: they showed that bacteria grow slightly faster in microchannels than in shaken Erlenmeyer flasks and that bacteria grow faster in smaller channels of oxygen-permeable PDMS up to a point at which the growth rate saturates at a certain surface-to-volume ratio of a channel, which has implications for microfluidic bioreactor design. Microfluidic devices can partition samples physically by directing portions of the sample from the main channel to separate chambers. This kind of separation is easy to achieve, and there are many approaches to filling such chambers. One of the earliest microfluidic devices with separate chambers was demonstrated in 2012,[67] and it contained 10 chambers of 1 μl volume each. The different antibiotic concentrations in each chamber were achieved by pipetting diluted antibiotic solutions into chambers before sealing the device. The solvent evaporated, and the device with chambers containing dried antibiotics was filled with a bacteria-containing growth medium. The chambers were then separated with oil and incubated to stimulate the growth of colonies, then the outcome was assessed visually. The approach of pipetting antibiotic solutions into chambers and then filling the chambers with the solution of bacteria to be separated in the chambers was firstly introduced[68] and then revisited recently with a 200-chamber device that was parallelized to form a
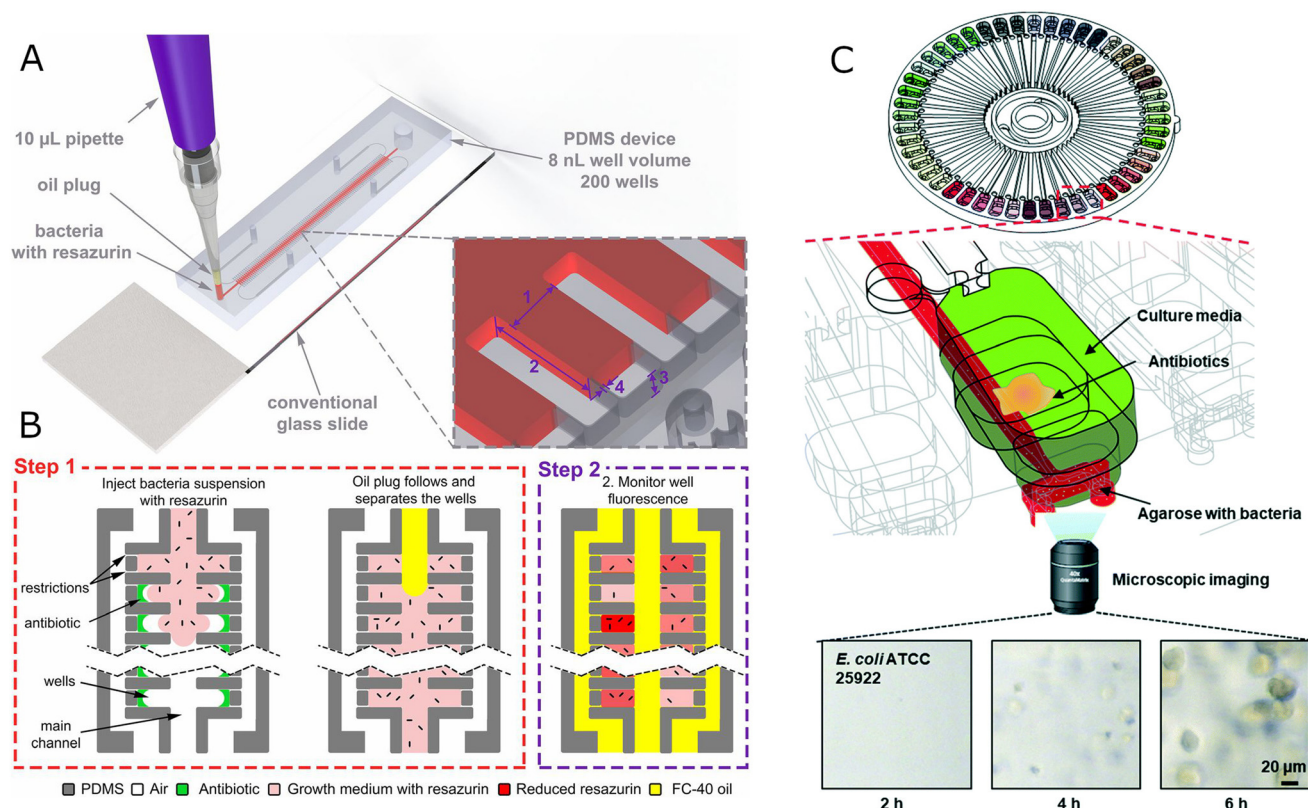
Fig. 2 Microfluidic static chambers for population-level studies. A) Schematic of the stationary nanoliter droplet array (SNDA)-AST system. The SNDA-AST device is placed on a standard microscope slide and operated by a 10 μl pipette. It consists of two rows of 8 nl chambers connected with the main channel delivering bacteria suspension or oil phase. Each well is equipped with 3 μm restrictions to let air escape to the surrounding channels. B) The SNDA-AST system is operated in two steps. In step 1, the device is loaded with a single-step injection of two plugs, bacterial suspension with 10% resazurin, followed by a plug of FC-40 oil. The oil separates the wells creating discrete, isolated chambers, delivering oxygen, and preventing evaporation. In step 2, the fluorescence intensity is measured every 30 min, which indicates the level of bacteria metabolic activity, and it is proportional to the amount of bacteria/metabolism in the chamber. Bacteria are not illustrated to scale. Reproduced from ref. 52. C) Schematic of a capillary and centrifugal-based AST (C2-AST) system containing dried antibiotics, agarose with bacteria, and culture media. The bottom time-lapsed microscope images show growing *E. coli* cells after 2, 4, and 6 h of incubation for left, central, and right images, respectively. Reproduced from ref. 60.

400-chamber microfluidic chip[69] that could, in principle, be multiplexed to house several sets of 200 wells per concentration of a drug. The flow of liquids in this solution is powered by a pipette, and the chambers are not dead-end (Fig. 2A and B), which brings a practical consequence: the filling of chambers is not based on degas pumping, where the chip is degassed so that when a sample is placed in the inlet of the chip, the chip that is expanding sucks the sample inside the chambers. A chip that does not rely on degassing does not require PDMS as the device's material. PDMS is famously expensive compared to thermoplastics (a kilogram of PDMS was *ca.* 50 times more expensive than a kilogram of polycarbonate or polymethyl methacrylate[70] which translates to $1–3 per PDMS microfluidic chip and $0.03–0.09 per polycarbonate microfluidic chip in materials costs), and it is challenging to produce PDMS devices on a mass scale. The described platform could, in principle, be produced with injection molding. A chamber-based device that allowed for dead-end chambers to be filled with a syringe was demonstrated,[71] although this solution allowed for testing of

only one concentration of antibiotic per device. Both platforms[69,71] relied on fluorinated oil to separate the chambers filled with resazurin, which might need consideration due to known leaking of resazurin to fluorinated oils.[72] In a modification of the established design, Lin *et al.* added microwells for bacteria to dead-end side chambers perpendicular to the main channel in which antibiotic gradient was generated.[73] The addition of microwells makes it possible to study isolated single cells in the device, however at a very limited throughput. The device was coupled with SERS for detection of bacterial growth.

Upscaling static chambers for MIC has to tackle the problem of multiplexing the assay. One of approaches to the issue is by serial dilution of the sample on chip, which was recently done by Osaid *et al.*, leading to an AST device integrated with a multiplexing module – this is a great feat of engineering; however, might be difficult to commercialize or use in clinic as the dilution module is rather complicated.[74] Further upscaling of chamber-based devices for AST resulted in systems containing over

1000 chambers.[75] Such an increase in throughput allowed for analysis of the efficacy of cocktails of antibiotics in search of synergistic, additive, or antagonistic relations. Pipetting over 1000 antibiotic samples into an array of microscopic wells is not feasible manually, so the authors used a droplet spotting machine. A spotting machine (a non-contact inkjet printer) allows for precise injection of very small volumes into wells that are microns apart from each other. However, such a machine is rather costly. If one were to commercialize such a system to put it to clinical use, they would need to consider the high maintenance cost of a spotting machine – this might be viable as the end chip is simple to use by non-experts. On the other hand, perhaps a different way of filling the chambers should be designed for commercialization, as PDMS used for degas filling of channels with oil to separate chambers is not ideal for mass production. It is possible to use syringes to generate suction within an array of chambers, and this approach does not necessarily require PDMS-made devices to work.[76] Another instance of prefilling microfluidic chambers with antibiotics and later filling all the chambers with bacteria was shown in a hybrid PDMS-paper device,[77] where small pieces of paper with antibiotic were placed in chambers before the experiment. Such an approach is undoubtedly more convenient than spotting the antibiotics to chambers with a spotting machine, and although only 21 chambers were placed in the device, the system was used to for breakpoint analysis of bacteria from clinical samples. In a separate approach, growth chambers were equipped with pressure valves that allowed for separate loading of chambers with bacteria and with antibiotic without drying the antibiotic, and antibiotic resistance of polymicrobial colonies was considered.[78,79] It is also possible to prepare a combinatorial gradient of antibiotic concentrations with microfluidic channels that allow for diffusion of different amount of antibiotic molecules into different regions of a hydrogel on which bacteria would grow – this simplistic approach could be applied to single-cell studies if bacteria isolating chambers were layered on top of the hydrogel.[80] Overall, the greatest scalability potential for microfluidic static chambers for AST lies in the antibiotic contact-free printing, even though this particular approach is technically demanding.

A distinct way of filling the chambers with a preloaded antibiotic was presented recently with centrifugal force within a lab-on-a-disc device.[81,82] With devices presented in both works, it was possible to prepare a series of chambers with a gradually changing antibiotic concentration and bacteria added separately to the antibiotic chambers (Fig. 2C). The devices are rather complex, with 3 layers of PDMS mounted on a plastic base. However, when assembled, these devices should be easy to use for an operator, as usual with the ab-on-a-disc technology. The samples in the systems are metered based on the size of metering chambers, which is advantageous due to high dosage precision of metering in

chambers, but might be limiting as the gradient (not the concentrations of antibiotic but rather the range of concentrations) is encoded in the device. This feature limits the flexibility of the device, but on the other hand, precise metering and reproducibility are desired when commercialization is considered.

2.2.2. Single-cell level studies in microfluidic static chambers. Microfluidics-based studies of single-cell growth in static chambers are relatively rare, although any static chamber device for population-level studies could be, in principle, repurposed for single cells. In a continuation to an agarose-based flow chamber system for AST[83] described in another section of this manuscript, Choi *et al.* further developed the design of the system and enhanced the imaging technique.[84] The system utilized a modified 96-well plate, each well containing two subwells in which bacteria in liquid agarose and antibiotics were added separately with a pipette. Agarose filled a microchannel that was placed around the antibiotic subwell, and monitoring of cell division was performed in agarose close to the antibiotic well. This design allowed for rapid preparation of an array of antibiotic concentrations in any desired concentration range, potentially also in antibiotic cocktails. The adaptation of a 96-well plate potentially allows to use commercially available pipetting robots to operate the device – at least with the dosing of the antibiotic solution, as robotic pipetting of liquid agarose might be challenging. The authors classify bacterial growth into 6 categories, including filamentous growth, *e.g.*, with β-lactam antibiotics with or without division, or swelling of cells. The authors' imaging algorithm distinguishes between, *e.g.* filamentous growth with or without division. This is important in establishing the MIC of Gram-negative bacteria with β-lactam antibiotics: cells that grow into filaments, but do not divide, increase the optical density (suggesting growth and resistance to the antibiotic), but as such cells do not divide (the antibiotic stopped their division), they should be considered susceptible to this antibiotic concentration. In their next system,[85] Choi *et al.* used a 96-well-plate-based design to assess the MIC of bacteria from clinical blood samples. The authors claim that in their system, they have not observed the inoculum effect (so that the MIC values were not influenced by initial bacterial density). However, the bacterial strains the authors used were later shown by different authors to exhibit almost no inoculum effect at all.[86] In the fourth publication in the series,[87] the authors used other strains to seek inoculum effect in their device, but they concluded that no inoculum effect is visible in their device, possibly due to very low initial cell density at which inoculum effect is generally not observed.[88] This feature would put the authors' system in the field of single-cell MIC (scMIC) measuring devices, not susceptible to significant MIC measurement errors stemming from the inoculum effect.[86] Another set of publications from the same group of authors describes their endeavors in assessing the MIC by following the morphology of

individual bacterial cells.[89–91] The authors correlate the length of cells with an antibiotic concentration in chambers placed atop electrodes that organize cells and allow for tracking specific organisms, showing good agreement with other AST methods.

A distinct technology for static chamber preparation relies on changes in the microchannel alignment after addition of subsequent reagents to the microfluidic device. This branch of microfluidics is called SlipChip and was first demonstrated in 2009.[92] SlipChip was used for AST based on blood samples and entropy-based image analysis of single cells allowed for assay results within 3–8 hours.[93] The applicability of this type of device is questionable for high throughput assays as leaks might be difficult to prevent while shifting two large plates with microstructures; however, smaller size SlipChips might be used in resource limited settings for their ease of use.

A distinct use of hydrogel trapping was demonstrated recently,[94] where authors formed dried hydrogel plugs that were placed in a conventional 96-well plate. Bacteria and antibiotics were pipetted to the wells causing the dried plugs to absorb liquid and swell, causing mechanical separation of individual cells at the bottom of the well. However, the gel is prone to antibiotic diffusion, so the separated chambers do not show an inoculum effect, which means that scMIC cannot be measured in the presented device.

An impedance-based device was used to track the growth of individual bacteria based on their motion within a closed microfluidic system. Bacteria would swim into a narrow channel, changing its effective channel diameter and the electrical conductance, resulting in voltage fluctuations.[95]

2.3. Microfluidic flow chambers for quantitative AST

In this section, we discuss microfluidic systems that separate the tested reaction conditions (antibiotic concentrations) for AST but that do not forbid the efficient exchange of medium. Such property is the effect of either culturing bacteria within a flow channel or by not adding long and narrow connector channels in between the device's main channel and the bacteria culturing chambers. Flow systems in which bacteria grow in the main channel are not often used for AST as the swimming bacteria are not shielded from the medium flow, meaning that the cells might be washed out of the chamber before the measurement is completed.

2.3.1. Population-level studies in microfluidic flow chambers. In an early application, bacteria bound to channel walls exhibited fluorescence only when an antibiotic killed the cells and allowed the fluorescent dye to bind to the nucleic acids.[96] A solution based on the classical microfluidic linear gradient generator[40] showed AST with bacteria growth measured by changes in turbidity within reaction chambers that were broader than the flow channel.[97] In another instance,[98] the linear antibiotic concentration gradient was formed by a flowing medium with antibiotic and a medium without antibiotic on two sides of a culturing chamber,

similar to the classical "Death Galaxy" device by Austin *et al.*[44] In this new solution,[98] bacteria grew within agar, which protected them from shear stress and from being washed away. The system was used for assessing bacterial growth in the presence of two antibiotics at different concentrations, which is advantageous as it allows for studies of antibiotic interactions, however the need for a syringe pump to be operating at a constant speed for the whole 6 h of measurement and the need for periodical refilling of media in device's reservoirs is limiting. A simple 8-channel device was used to compare the antimicrobial activity of a library of peptides, showing difference to the activity of same compounds when tested in a well plate, and suggesting that the choice of materials for a microfluidic device is critical.[99] A separate approach in which the resistance or susceptibility was determined by counting the number of dead bacterial cells was shown in a simple microchannel device.[100]

2.3.2. Single-cell level studies in microfluidic flow chambers. Measuring AST is usually associated with either observing directly the growth of a colony or with following indirect signals coming from a growing bacteria colony. Tracking divisions of individual cells was suggested as the ultimate fast phenotypic AST method, and, indeed, the results of an AST are achievable even within 30 minutes with this approach. The technical problem connected with imaging individual cell division is that swimming bacteria are difficult to follow in a culture chamber. The solutions to this issue that have been suggested include electrophoretic ordering of cells or mechanical immobilization of cells either in separate microchambers or within agarose gel. The first example of AST based on tracking individual cells in a flow chamber contained only a single microfluidic channel with an array of electrodes for bacteria ordering.[101] This is probably the first report on the inoculum effect in microfluidic devices (see the "inoculum effect considerations" section below).

One of the most prevalent microfluidic single-phase designs for microbiology is the mother machine,[102] which has been used on numerous occasions to study bacteria in an antibiotic context or close to it: *e.g.*, mother machine was used for the analysis of mutation frequency in *E. coli*,[103] for studying viable but non-culturable bacteria during antibiotic treatment,[104] for describing the accumulation of polar multidrug efflux pumps that grant antibiotic resistance in older cells and less so in daughter cells,[105] for studying bacterial persistence,[106,107] uptake and efflux of antibiotics by bacteria[108] with fluorescently labelled antibiotics,[109] and measuring the efficacy of bacteria clearance with phages.[110,111] The basic mother machine consists of a large main channel through which growth medium flows and of multiple shallow and narrow dead-end channels that are perpendicular to the main channel, forming a comb-like structure. The bacteria are placed in the main channel, and they fill the shallow channels one by one. When a sufficient number of channels contains a single cell, the flow is changed to a bacteria-free medium in the main channel. The
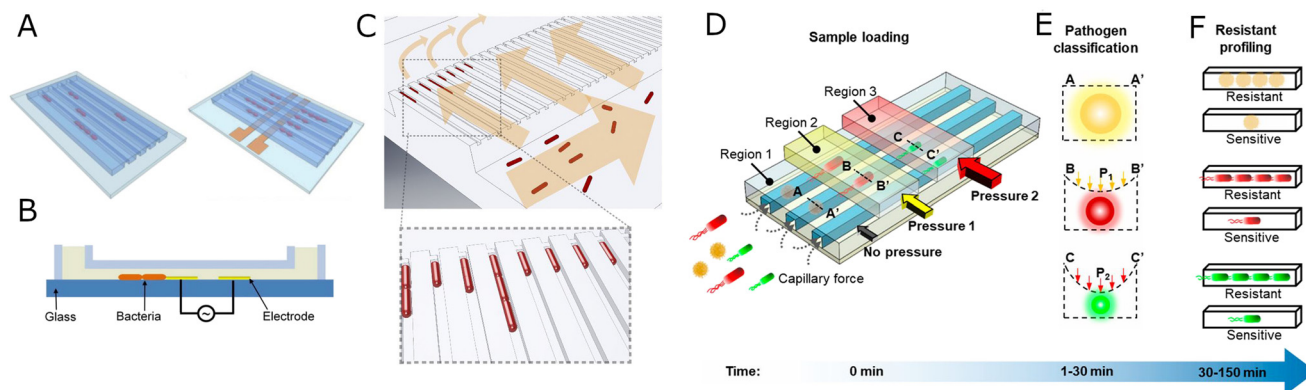
Fig. 3 Evolution of mother machine systems. A) Electrode-based ordering of bacterial cells. Schematic representation of bacteria trapping in microchannels for single-cell AST without (left) and with electrokinetic positioning (right). B) A cross-section view of the microchannel with a pair of electrodes for bacterial cells (orange) trapping by dielectrophoretic force. A and B reproduced from ref. 81. C) Sieve-like design of the mother machine. Bacteria (red) are loaded from the front channel, and they are prevented from passing to the backchannel by a constriction at the end of each trap. The arrows indicate the direction of flow during chip loading. Reproduced from ref. 82. D) Adaptable mother machine system for bacteria identification and AST. Bacteria are loaded into region 1 (undeformed) and regions 2 and 3 (differently deformed with pressure) of the channels automatically by capillary force. Pressure might be applied to channels marked as regions 2 and 3 to deform the bacteria channels and to sieve out cells of different size. E) A cross-section view of microfluidic channels with trapped bacteria under different pneumatic pressures. The cells are trapped in different regions of microchannels and classified according to the applied pressure. A, A′, B, B′, C, C′ – positions in the bacteria channel profiles as seen in D. P_1, P_2 – different pressures used to deform the bacterial channels. F) Bacteria susceptibility to antibiotics is assessed by monitoring bacteria growth in the presence of antibiotics. D–F reproduced from ref. 83.

bacteria at the dead ends of narrow channels divide, and their daughter cells move closer to the main channel and are eventually washed away, but the mother cell at the dead-end of a shallow channel does not move. The first use of the mother machine in AST was presented by Lu *et al.* where the authors positioned the bacteria in the shallow channels electrokinetically, so that the bacteria are always lined up next to an electrode, which facilitates optical imaging[112] (Fig. 3A and B). The authors followed the length of colonies in time (growth rates) in channels starting from a single cell and analyzed the growth rate changes in the presence of antibiotics, and showed that MIC could be determined within one hour in their system. They also demonstrate distributions of growth rates within a population of bacteria when untreated or treated with an antibiotic. Baltekin *et al.* elaborate on this solution by following the growth rates of individual bacteria at a large scale in populations (Fig. 3C) where antibiotic was added to the flowing medium and compared the measured values to growth rates of cells in antibiotic-free conditions. After 30 minutes, the authors were able to determine with high confidence that a given strain is either susceptible or resistant to a given antibiotic in a given concentration.[113] Li *et al.* used a similar approach and also measured growth rates (or lengths of bacterial colonies formed in an individual microchannel), but they also implemented channels perpendicular to shallow bacteria channels on top of the shallow bacteria channels[114] (Fig. 3D). These top channels resemble a classical microfluidic module called Quake valves (in memory of the inventor):[41] the top channel is pressurized, and the PDMS layer between the top channel and bottom channel deforms as the pressure is applied to the top channel (PDMS is elastic). Higher applied

pressure means larger deformation of the channel, and, consequently, smaller height of the bottom bacteria channel. This behavior was used by Li *et al.* to stop bacteria of the desired size in the bottom channel through trapping the cells with the controlled channel height. The separation of differently sized cells allowed the authors to identify the trapped bacteria species from a sample (Fig. 3E). Size-based differentiation of the most common infectious agents might be helpful when planning an antibiotic therapy or tracking the infection onset (Fig. 3F).

In a separate effort to study antibiotic resistance by tracking divisions of single cells in a microfluidic device, Choi *et al.* and then Jung *et al.* presented a series of fast AST solutions based on tracking divisions of individual cells immobilized in agarose.[83–85] The first iteration of their system is a flow chamber: Choi *et al.* had prepared a channel that they filled with bacteria in liquid agarose, and after the agarose solidified, a solution of antibiotic in a culture medium was injected into a side channel of the system, leading to diffusion of the antibiotic from the solution into the agarose pores. The authors then imaged the neighborhood of the side channel and assessed the growth of bacteria. The device was multiplexed into 6 sets of channels and side channels – this allowed for AST of 6 antibiotic concentrations at once. This system was rather complicated, and it required a syringe pump to be dosing antibiotics during the whole experiment. Another group of authors used a simple agarose-based diffusion design to generate an antibiotic concentration gradient and correlate the cell length with the antibiotic abundance,[115] an approach similar to another microfluidic AST solution.[90] They pointed to heterogeneity in cell length at intermediate antibiotic

View Article Online

Lab on a Chip

antibiotics. The bacteria attached themselves to the bead, changing its rotational frequency. At a sufficiently high antibiotic concentration, there were no bacteria to reduce the rotational frequency, and MIC was thus established. Amselem et al.[119] developed a system in which a gradient of concentrations is established by diffusion during the laminar flow of antibiotic containing liquid parallel to an antibiotic-lacking medium, similarly to solutions presented in single-phase microfluidic systems. In their system, Amselem et al. used a chamber with 1500 wells filled with a bacteria solution. Then the chamber was filled with oil that separated the wells, trapping individual droplets with bacteria in the wells (Fig. 4A–C). The device works with either liquid droplets for swimming bacteria or with gel beads for immobile colonies. The dynamic range of this system is limited. However, the authors later presented a modification of the system that allows for firstly trapping droplets of one sample and then adding precisely measured portions of another sample to the trapped droplets[120] – one can imagine using such a modified platform to run AST with a broad dynamic range by firstly trapping droplets with bacteria and then adding droplets of pre-diluted antibiotic. Sabhachandani et al. demonstrated a droplet array for AST with such a pre-dilution where they trapped 1000 small droplets (1 pl to 10 nl). The droplets were generated with an embedded flow-focusing geometry, and the droplets were later imaged on a chip (Fig. 4D and E). The device integration is similar to the work of Amselem et al.[119] A redesigned system of Sabhachandani et al.[121] was demonstrated by researchers from the same laboratory as Kang et al.,[122] where the authors use a device with 4 arrays of 8000 droplets each for AST and find subpopulations of highly resistant bacteria. The device is scalable, so it is possible to house more antibiotic concentrations on a single chip. However it would require more inlet and outlet ports, making the device relatively complex. An easy-to-use device for AST in droplet arrays was presented by Kao et al.[55] The authors used a passive method of generation of droplets (microfluidic step emulsification[123]) to emulsify samples that had been pipetted on the chip. Each sample (bacteria with added different concentrations of antibiotics) was emulsified to a separate chamber with emulsification driven by gravity, thus making the system relatively cheap (no pumping setup for flow control) and easy to operate. The platform relied on fluorescence readout, thus limiting its clinical application. Derzsi et al. developed a system in which the antibiotic dilution series was prepared in droplets on a chip passively and merged with bacteria droplets also prepared passively on the same chip. The passive nature of the assay was possible due to special engineering of the microfluidic channels and allowed for preparation of a microdroplet-based AST in five pipetting steps.[124] This system could in principle be used for single cell studies, however the small number of assayed droplets limits the information gained in the experiments. All the droplet arrays described to this point relied on separate droplet chambers for each antibiotic concentration. In a system

developed by Kulesa and colleagues,[53] the authors applied a method known as 'color coding':[125] Kulesa et al. used combinations of three fluorescent dyes that emit fluorescence at distinct wavelengths to mark droplets with different antibiotic concentrations – each concentration received a unique set of concentrations of dyes (Fig. 4F). This approach allowed the authors to pool the droplets into one large droplet array, thus significantly reducing the engineering complexity of the assay, on the other hand making the optical analysis more complex. However, once the image analysis protocols were established, the authors were able to use this platform to assess dose–response interactions of 10 antibiotics with over 4000 adjuvants. The authors studied only populations of cells trapped in droplets, however single-cell analysis in their device is feasible.

2.5. Flowing droplets for quantitative AST

A separate category of microfluidic devices is based on droplets generated at high throughputs and collected for incubation in a test tube. After incubation, the droplets can be moved to a detection system, where they are scanned for optical signals at hundreds or thousands of droplets per second. Contrary to the droplet array systems described above, none of the systems based on the analysis of flowing droplets can be used for rapid AST based on tracking divisions of individual cells. This stems from the fact that the optical read-out of bacterial growth in flowing droplets is an end-point measurement – it is until now not possible to conveniently track thousands of individual droplets in an emulsion for hours to check if bacteria in a given droplet are dividing – such tracking was done only for at most hundreds of large (hundreds of nanoliters) droplets.[126,127] Jakiela et al.[128] presented the first droplet system supporting chemostat-like conditions for long-term incubation of bacteria and demonstrated the use of this system in tracking adaptation of bacteria to antibiotics. Apart from that, the bacteria in droplets need culturing so that the optical signal from droplets is strong enough to be detected. This instantly leads to a conclusion that systems based on flowing droplets are not suited for clinical practice as they cannot inform a diagnosis as rapidly as the systems for immobile bacterial cultures. Flowing droplet systems, however, offer large scaling possibilities, which we discuss in the 'opportunities' section.

The flowing droplets can be used for single-cell level analysis: firstly, one needs to stochastically confine cells in droplets so that each droplet contains at most a single cell; then, after incubating the emulsion, the colonies formed in droplets from single cells are detectable. This was first demonstrated by Boedicker and colleagues[129] when the authors prepared multiple series of 50 droplets, each droplet 1 nanoliter in volume, each series of droplets with different antibiotic concentrations. The droplet series were separated from each other in a piece of tubing with air bubbles. Due to stochastic confinement, only a few of the 50 droplets per

This journal is © The Royal Society of Chemistry 2022
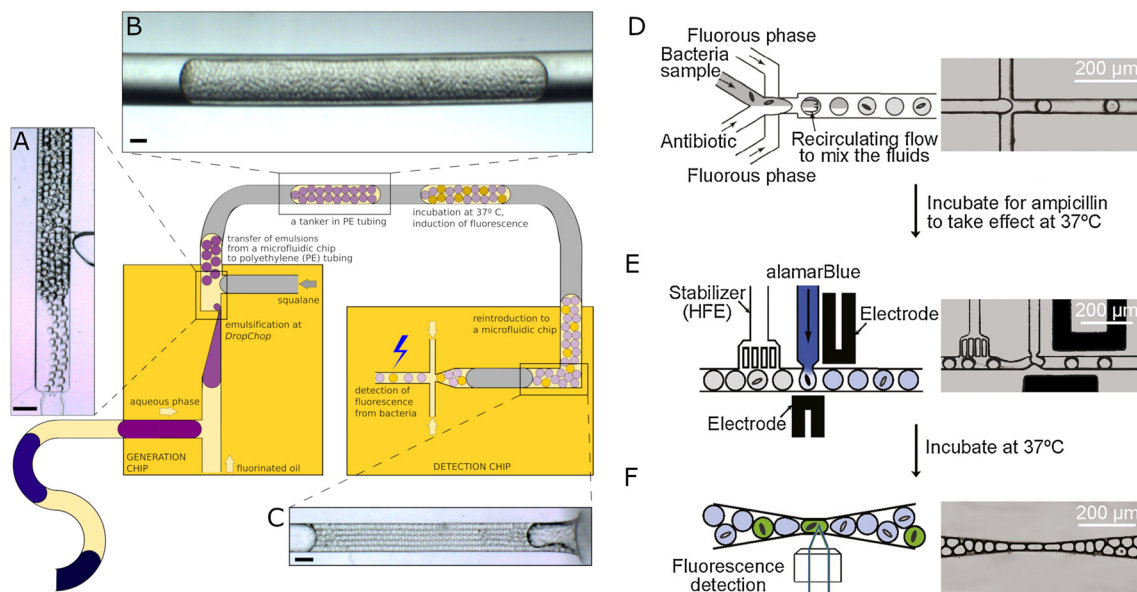
Fig. 5 Antimicrobial susceptibility testing using flowing droplet systems. A–C) Semi-automatic droplet-based system for single-cell AST. Large droplets containing bacteria and various antibiotic concentrations generated before with T-junction or through aspiration by a positioning system for tubing are split into nanoliter droplets using vertically oriented *DropChop* emulsifying geometry (A). The subsequent libraries are separated by immiscible squalene oil (gray) and collected in PE tubing (B). The emulsions (tankers) are then incubated to allow bacteria to grow and increase the droplets' fluorescence intensity, which is measured in the detection chip after incubation (C). Scale bars: 400 μm. A–C reproduced from ref. 96. D–F) Droplet-based method for single-cell quantification of phenotypic heteroresistance. Bacteria sample with an antibiotic is split into droplets (D) and incubated at 37 °C. After incubation, the droplets are reintroduced to the microfluidic device. A viability probe alamarBlue is pico-injected into each drop I), and the droplets are collected for additional incubation. In the last step, the fluorescence intensity is registered in each droplet, and the heteroresistance of the bacterial population can be quantified. D–F Reproduced from ref. 99.

antibiotic concentration contained cells, so the throughput of the method was limited. The throughput of this method was improved a decade later by Postek *et al.*, where authors were able to semi-automatically generate dozens of emulsions of *ca.* 2000 droplets each where each emulsion contained a different antibiotic concentration[130] (Fig. 5A–C). In single-cell level experiments by Postek *et al.*, a single emulsion contained *ca.* 200 droplets with individually encapsulated bacteria inside, opening possibilities for studies of population heterogeneity in isolated cells. A system similar to that of Postek *et al.*[130] was presented recently with a different approach to droplet generation and emulsion handling.[131] Single-cell level studies have also been performed in droplets by Liu *et al.*,[132] Lyu *et al.*,[133] Scheler *et al.*,[134] and Kaushik *et al.*[135] Kaushik and colleagues manually (in a non-automated fashion) generated emulsions with different antibiotic concentrations and with single cells encapsulated in droplets, then measured end-point signals from droplets to establish whether the cells grew or not. Scheler *et al.* run similar experiments, however, on a larger scale: to identify emulsions with different antibiotic concentrations after pooling the droplets, the authors color-coded them before pooling the droplets for incubation and detection.[134] The authors demonstrated that individual bacteria within an isogenic population have different levels of antibiotic resistance. Liu *et al.* also generated droplets with bacteria and antibiotics manually, incubated each emulsion with different antibiotic concentrations in separate test tubes, and

later performed a high-throughput measurement of optical density inside droplets to verify if a given droplet contained growing bacteria.[132] As optical density was screened, this technique is suitable for testing the resistance of clinical strains of bacteria. Lyu *et al.* used a similar strategy of manual emulsion generation[133] (Fig. 5D–F). After incubation, the authors used a pico-injector[136] to seed each droplet with a dye resazurin to detect fluorescence from droplets containing living cells. As the authors generated 10^7 droplets per antibiotic concentration, they were analyzing 10^6 individual bacteria per antibiotic concentration, thus being able to identify rare resistant subpopulations of cells.

In population-level studies, Funfak *et al.* demonstrated a system in which the authors screened for bacterial response to toxins by inserting pH-sensitive polymer sensor particles in droplets with bacteria and tested compounds.[137] Churski and colleagues[138] demonstrated an automated system for the generation of gradients of two antibiotics in droplets with the addition of bacteria to each droplet. The authors used the device to screen for interactions between antibiotics in multiple concentrations at a narrow concentration range. Due to the technical aspect of droplet generation, this particular solution is not fit to screen broad concentration ranges, limiting its use in medical diagnostics. In a different approach, Baraban *et al.*[127] and Jiang *et al.*[139] demonstrated platforms that use droplets of 100 nl or 1 nl, respectively, to screen for MIC. Baraban *et al.* used a system with 1000 media droplets of 100 nl each, each droplet being separated from its

neighbor media droplets by a portion of mineral oil. This indexing of droplets in a piece of tubing is the same as in the earlier work of Boedicker *et al.*[129] and later by Churski *et al.*,[138] Postek *et al.*,[130] and Li *et al.*[131] Apart from establishing MIC with a fluorescence-based detector, Baraban *et al.* measured the saturation number of bacteria per droplet volume, being 27×10^4 cells per 100 nl droplet for the conditions used. The authors showed that their platform is more precise than a gold standard platform for clinical AST, the VITEK® 2 by bioMérieux,[139] due to the large numbers of droplets screened per single experimental run. Jiang *et al.*[139] used resazurin fluorescent dye, which allowed the authors to expand to clinical strains. However, resazurin does not work with anaerobic bacteria. Both systems by Baraban *et al.* and by Jiang *et al.* suffer from a narrow range of antibiotic concentrations that can be tested due to technical limitations of the droplet generation method used – in the same way that limited the system by Churski and colleagues.[138]

3. Signal detection in microfluidic AST

Here we describe the methods of bacterial growth detection in microfluidics in the context of AST. We focus on the two methods we find the most important: i) optical detection which is still the golden standard in the clinic; ii) pheno-molecular detection which combines uses quantitative measurements of bacterial nucleic acids as a proxy for cell growth, and is a major improvement over classical molecular AST detection assays. The only assay covered in this review that produced AST results within 30 minutes of the patient sample collection is pheno-molecular. We also highlight other important methods of bacterial growth detection that were used in microfluidic AST and show promise in cutting the signal detection time.

3.1. Optical detection of bacterial growth for microfluidic AST

Eucast[140] and CLSI[141] are both recommending that an inoculum (bacteria density) of 5×10^5 CFU ml^{-1} should be used in an AST assay. This brings up a problem of the inoculum effect discussed later in this article. However, the inoculum recommendation also means that AST is generally measured for a population of cells. Studying whole populations masks the effects that might arise from a single mutated cell or a small set of interacting cells, such as perister cells[142] or viable but non culturable bacteria.[104] On the technical level, testing large numbers of bacteria implies relatively easy use of optical detection of signals: as the test subjects are numerous, the signal produced by the bacteria population is high compared to the background. It is possible to run AST coupled stimulated Raman scattering[143] for detection. Analysis of metabolism[143–145] allows for AST within 30 minutes or within 2–3 hours by measuring the dissolved oxygen levels in a bacteria sample during cultivation[145] by tracking luminescence of oxygen-sensing probes.

3.1.1. Fluorescent markers. For research purposes, it is possible to use fluorescent protein markers encoded in the bacterial genome to analyze the MIC levels. However, in a clinical setting, this is out of the question as patient samples usually do not contain fluorescent proteins. Use of metabolism markers such as resorufin/resazurin is possible; however, their use is limited to closed microfluidic chambers or to droplets in which a problem of leakage from droplets to surrounding oil might reduce the precision of an assay.[72,146,147] We have highlighted the problem of contamination between droplets in our previous article,[148] and since then, the leakage problem has been targeted by designing new surfactants.[57] Leakage of small molecules is important not only because of retention of fluorescent dyes but because the leakage may also include the transfer of antibiotics between droplets. The main means of transport of matter between droplets in a surfactant-stabilized emulsion is by the detachment of minuscule droplets from one large droplet and attachment of these small droplets to another large droplet – such a mechanism does not require the leaking molecule to diffuse from a droplet to surrounding oil to contaminate other droplets and thus might apply to hydrophilic molecules.[149] Resazurin is a marker of the respiratory activity of a cell, thus, resazurin is not compatible with anaerobic bacteria. We suggest that resazurin should not be a marker of choice for the detection of bacterial growth in clinical samples, and other label-free techniques should be applied.[150]

3.1.2. Optical density. The problem with OD analysis is the extended time – typically of few hours – that is necessary for the bacterial colony to grow sufficiently to produce a detectable signal. There are ways around this problem, such as monitoring divisions of individual cells[113] to allow for measurements of MIC within tens of minutes, which, however, limits the scale of the assay. The main challenges with detecting bacterial growth by monitoring divisions of single cells are the cost of the optical components of the setup, possible problems with tracking motile bacteria and scaling up the detection to monitor multiple cells in multiple reaction compartments (different antibiotics at different concentrations). Droplet arrays might provide for multiplexed rapid ASTs, where single-cell level growth monitoring in droplets is required. One study covered here showed such a feat in a droplet array at low throughput,[121] but progress in this direction is being made by, *e.g.*, applying smartphone cameras to detection of bacteria growth in single phase microfluidic devices[151] or in droplets,[152] albeit in this piece of research, it took 6 hours until the bacteria in droplets grew dense enough to be detected. Single-cell level growth detection is also developed with fluorescent cells.[153] In a recently published report Taylor *et al.* report counting individual cells with no fluorescent markers in arrays of 1000 droplets each.[154]

OD-based bacterial growth detection in flowing droplets is under development as well, and the first deployed systems promise good prospects for AST measurements of clinical samples in droplets.[155] The first reports on label-free detectors of bacterial growth in droplets concern large compartments of *ca.* microliter volume[126,156] – such volumes do not allow for

high-throughput applications, which is the greatest advantage of droplet-based systems. High-throughput screening requires using small droplets of the order of nanoliters and smaller. Boitard and colleagues presented a method for bacteria growth detection in picodroplets based on the change of osmotic pressure and the droplets' size due to bacteria growth,[157] although this method does not provide high-throughput droplet analysis. Similarly, Liao et al. showed an exciting approach for label-free and sensitive detection of bacterial cells in picodroplets using micro-Raman spectroscopy, but without the possibility of high-throughput droplet screening.[42] More promising approaches are presented by Zang et al., who showed bacteria detection based on real-time image processing at a frequency of 100 Hz,[158] and by Liu et al., where the measurement relies on detecting light scattered by bacterial cells at a frequency of 243 Hz.[132] Similarly, Hengoju et al. showed an optofluidic detection system based on absorbance readout and scattered light in picoliter droplets with a frequency of approx. 40 Hz.[155] The highest throughput of screening of droplets containing bacteria for bacteria growth to date was presented by Pacocha et al., where the growth of bacteria based on the intensity of scattered light was measured at a frequency of 1200 Hz, promising good prospects for AST measurements of clinical samples in droplets. We see flowing droplets not as tools for clinical use, but rather for academic research, and the throughput of signal detection from flowing droplets is not critical for non-clinical ASTs.

3.2. Pheno-molecular detection of bacterial growth for microfluidic AST

Molecular methods are a promising path in microfluidic AST development: molecular tests can identify a pathogen, verify if it is resistant to an antibiotic, and finally measure the MIC of a given antibiotic with the identified bacterium, also at the single-cell level. The molecular AST in microfluidics stems from digital PCR:[159,160] similarly to confining individual bacteria in droplets, a sample containing multiple DNA target molecules can be divided into numerous separate droplets, so that each droplet contains either no DNA molecules or at most a single DNA target molecule.[59] Then the amplification is performed as in classical PCR. The answer is a signal coming from only the droplets that contained DNA. Since each droplet stored at most one DNA molecule, counting the compartments that provide a positive signal allows counting the number of DNA molecules before the reaction with absolute precision and without the need for calibration curves as in real-time PCR. Molecular detection of antibiotic resistance is applied to microdroplets;[161] however, the issue in incorporating molecular tests to AST is that the lack of resistance genes is not a reliable predictor of susceptibility to a given antibiotic[162] apart from a few resistance genes (e.g., mecA, vanA, vanB[163]), which is why the hybrid phenotypic–genotypic approach ("pheno-molecular", as called by Athamanolap et al.[164]) was developed. This hybrid approach uses the number of DNA or RNA molecules in the sample as a proxy for the growth of bacteria. The founding research for

microfluidic pheno-molecular AST was published in 2015 by Hou et al.,[165] who used inertial microfluidics to separate bacteria from whole blood samples and screened with non-enzymatic nucleic acid detection assay (NanoString) for antibiotic-response-related mRNA. A first DNA-based pheno-molecular assay was presented in 2016 by Schoepp and colleagues,[166] where authors compared the changes in concentration of pathogen-specific DNA sequences after exposure to antibiotics. The resistant bacteria would show similar DNA concentrations over time in both antibiotic-treated sample and in antibiotic-free control, while susceptible strains would show a slower increase or no increase in DNA concentration in a treated sample when compared to an antibiotic-free control. The authors demonstrated that droplet digital PCR allows for faster detection of changes in concentration of pathogen-specific DNA after exposure to antibiotics compared to qPCR. In their subsequent development, Schoepp and colleagues[167] optimized the droplet digital LAMP (loop-mediated isothermal amplification[168]) reaction, the sample handling protocol, and the signal detection software so that they were able to distinguish between antibiotic-susceptible and antibiotic-resistant bacteria from unprocessed clinical samples within 30 minutes (Fig. 6A–D). The detection this fast is impressive as even the fast optics-based AST methods that follow individual cells are slower than the presented method. The same group later showed that it is possible to rapidly identify antibiotic-resistant or susceptible slow-growing bacteria by measuring the levels of the RNA markers of bacteria exposed to antibiotics[169] – possibly, this or another research team will try and run such RNA measurements with clinical samples as well. Athamanolap and colleagues developed a system for pheno-molecular AST based on 5000 1 nl wells for partitioning the sample instead of using droplets[164] (Fig. 6E). The authors analyzed DNA melt curves from each well and used machine learning to teach their program to distinguish between species-specific melt curves. The number of species-specific melt curves was counted and compared between samples treated and untreated with an antibiotic to identify antibiotic susceptibility, albeit slower than in the report by Shoepp and colleagues. Kaushik and colleagues used a pheno-molecular approach to identify if bacteria from urine samples are E. coli, Enterobacteriales but not E. coli or non-Enterobacteriales Gram-negative cells. Additionally, the authors analyzed the antibiotic resistance of the tested cells by merging PNA fluorescent probes for 16S RNA with fluorescence detector. The system was shown to identify bacteria and their antibiotic resistance from urine samples in 30 minutes[170] (Fig. 6F–H).

3.3. Mechanical detection of bacterial growth for microfluidic AST

Mechanical detection of bacterial growth in microfluidics is done with cantilever sensors that resinate at different frequencies depending on the cantilever mass. The cantilever mass is changed when bacterial cells are added to the sensor.[171–176] Microfluidic cantilever-based sensors[173] allow
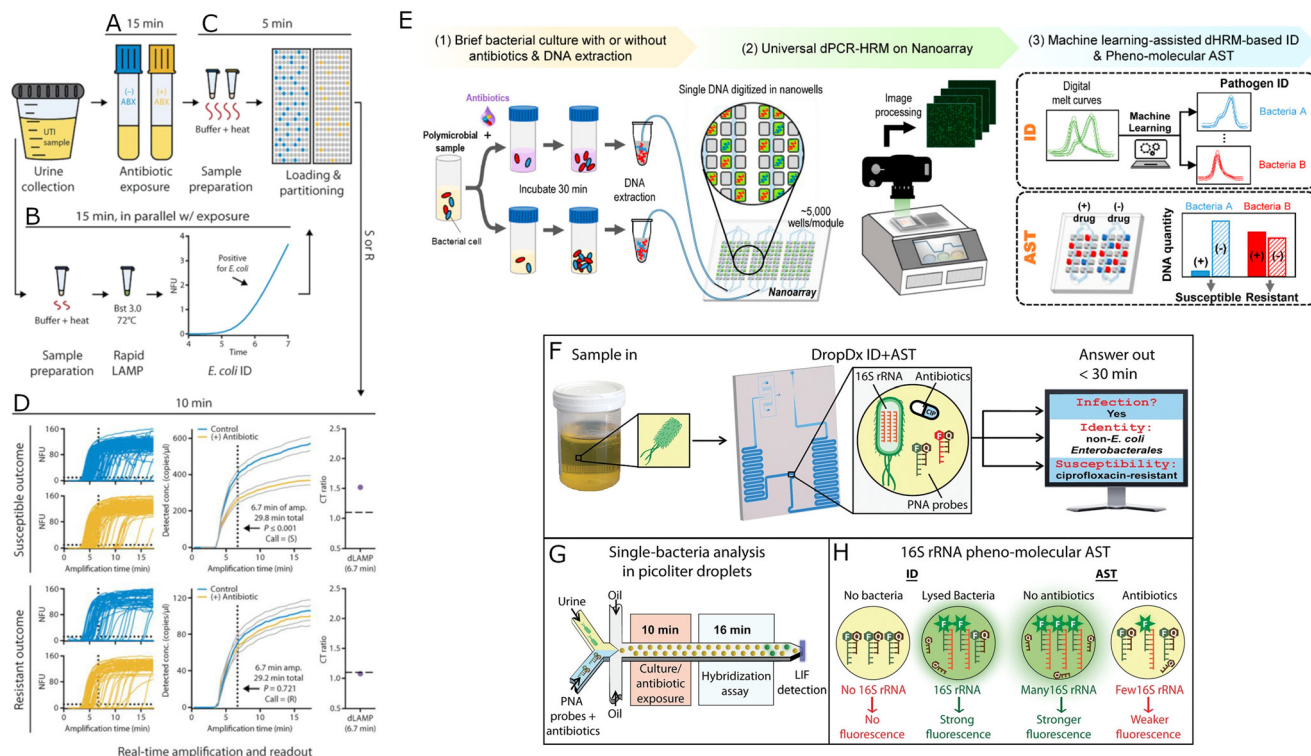
Fig. 6 Microfluidic pheno-molecular AST assays. A–D) Phenotypic susceptibility testing using digital LAMP quantification. The UTI (urinary tract infection) sample is incubated in the presence and absence of antibiotic for 15 min (A). In parallel, the nucleic acids (NAs) prepared from an aliquot of the urine sample are amplified by bulk LAMP assay indicating *E. coli* at clinically relevant concentrations (B). Then, NAs are extracted from control and antibiotic-treated samples using extraction buffer and partitioned using SlipChips for dLAMP quantification (C). The process of NAs amplification is monitored in real-time, and after 6.7 min, the susceptibility can be determined (D). The presented data concerns one resistant and one susceptible bacteria. Gray lines represent 95% confidence intervals. A–D Reproduced from ref. 113. E) Digital PCR and melt platform for rapid bacteria identification and AST. The workflow starts with the incubation of bacteria with and without antibiotics for 30 min. Bacterial DNA is extracted from both samples, mixed with a universal PCR mixture, and loaded into a nanoarray device for dPCR-HRM (digital PCR and high-resolution melt). Then, the 'temperature lapse' fluorescence images are analyzed, and digital melt curves for all nanowells are created. Bacterial species are identified using a machine-learning-based melt curves identification algorithm. The DNA copy number is determined by enumeration of species-specific digital melt curves. Finally, the antibiotic susceptibility is assessed by comparing the DNA copy numbers of both samples (treated and not treated with antibiotics). Reproduced from ref. 110. F–H) Droplet-based pheno-molecular ID and AST of UTIs. The system allows for a single-cell detection of 16S rRNA, providing confirmation of Gram-negative bacterial infection, uropathogen identification, and determination of its antimicrobial susceptibility (F). Urine sample, 16S rRNA-specific fluorogenic PNA probes, and/or antibiotics are split into picoliter droplets. Then, bacteria are exposed to culture or antibiotic for 10 min followed by a probe hybridization process for 16 min, and target a two-color laser-induced fluorescence (LIF) detector (G). The identification of uropathogenic bacteria is based on detecting specific 16S rRNA sequences using the fluorescence color and intensity of droplets. The difference in probe fluorescence intensities between antibiotic-dosed and antibiotic-free droplets is used to measure the relative production of 16S rRNA in single cells, which is used to determine antimicrobial resistance. F–H Reproduced from ref. 116.

for determining antibiotic resistance within 45 minutes,[174] which is short enough time to validate deployment of the method to the clinic. There are start-up companies such as Resistell that are exploiting cantilever-based sensors in their products for AST.[27] There is a recent review article available focusing on mechanical detection of bacterial growth for AST and we direct the reader there for more information.[177]

3.4. Electrical detection of bacterial growth for microfluidic AST

Electrical impedance measurements for fast detection of bacterial growth has been a viable concept for many years.[178] The advantage of electrical signal detection over the optical or molecular detection methods is the fact that no expensive miscroscope or no expensive molecular biology reagents are

necessary for AST. In the past decade, the electrical detection of bacterial growth has been adapted to microfluidics, leading to rapid detection times.[95,116,179] The electrical resistance of the microchannels change in proportion to the number of bacteria in the microchannels. Optimal electrode placement around a microchannel in a impedance micro-cytometer have allowed for identifying susceptibility or resistance in *ca.* 30 minutes[180] after analyzing *ca.* 1000 cells per second. Microfluidics impedance cytometry was recently covered in an informative review article.[181]

3.5. CRISPR detection of bacterial growth for microfluidic AST

Here we mention molecular (not pheno-molecular detection) of bacterial growth that is based on a CRISPR screen.

Recently, CARMEN, an assay based on SHERLOCK[182] was demonstrated in droplets to differentiate viruses from a vast collection of 169 human-associated viruses.[183] A modified CARMEN assay was deployed to identify 52 clinically relevant bacterial pathogens in a single assay with additional identification of major antibiotic resistance genes.[184] Although this assay is molecular, not pheno-molecular, it could in principle be combined with a pheno-molecular approach to achieve a platform that would both identify a pathogen and also rapidly establish the pathogen's antibiotic resistance levels – which is the holy grail of clinical AST.

4. Challenges and opportunities

4.1. Challenges

4.1.1. Detection time. The outcome of phenotypic AST is the bacterial state after exposure to the antibiotic, the phenotype being growth or no growth of cells. It might take more than a day for slow-growing bacteria to be detectable as they need to divide enough times to become visible under a microscope. There are two main approaches to the issue of detection time in microfluidic AST, and they both come with their own challenges.

The first main approach is to follow the growth of individual cells in the presence of antibiotics. It has been shown that such tests can provide MIC rapidly, even within 30 minutes[113] with clinical isolates (not with clinical samples). However, approaches based on single-cell imaging require high-resolution optics and time-lapse imaging of multiple locations, which makes these methods expensive and, until today, unfit for clinical practice.

Another major approach to reducing detection type is "pheno-molecular" assays, where methods of nucleic acid quantification are used to quantify the number of DNA or RNA of interest in the bacterial lysate. The DNA/RNA molecule count is a proxy for bacterial growth and has been shown to be faster than optical growth-based assays, even for analysis of clinical samples such as urine (not the bacteria isolates from such samples).[167] There are other paths to run rapid ASTs in microfluidic devices: analysis of metabolism[143–145] allows for AST within 30 minutes, albeit with expensive stimulated Raman scattering,[143] or within 2–3 hours by measuring the dissolved oxygen levels in a bacteria sample during cultivation;[145] microfluidic cantilever-based sensors[173] allow for determining antibiotic resistance within 45 minutes.[174] A microfluidic impedance-based assay was demonstrated recently, identifying susceptibility or resistance in *ca.* 30 minutes.[180]

Obtaining AST results within 30–60 minutes from a clinical sample (not bacterial isolate: isolates require additional time to prepare) is enough for a physician to inform the patient of the nature of an infection during a single visit, and we do not see any need to improve on the detection time below what has already been shown. At the time of writing of this article, only microfluidic pheno-molecular assays were shown to achieve AST results from clinical samples in such a short time; however, optical or sensor-based based microfluidic methods are lagging not far behind.

4.1.2. Multiplexing. A major hurdle now would be to develop multiplex AST assays so that the test results are comprehensive, *i.e.*, they inform about susceptibility to multiple antibiotics, possibly with an MIC screen instead of a breakpoint analysis.

4.1.2.1. Printing antibiotics. From systems that follow single cell division presented to date, only one is capable of multiplexing for many antibiotics or many concentrations of antibiotics per experimental run,[84] and this is because the test is based on a modified 96 well-plate. Similar multiplexing could be easily achievable with chamber-based devices where antibiotic is placed into chambers and dried before the bacteria sample is flown through the device and segmented into chambers. Both of these approaches are possible to automate with either pipetting robots for 96 well-plates or with spotters (droplet printers) in case of drying antibiotics on chips. The well-plate method, however, requires the application of the sample separately to each well, therefore automation could only be done with the help of a specialized diagnostics facility, which is counter to the commercial goal of point-of-care microfluidic ASTs. Printing antibiotics into chambers is more difficult technically than pipetting samples to well-plates, as the chambers are usually much smaller than wells. However, the to-date presented chamber-based solutions require the end-user to perform only a single pipetting step or two steps at most to run AST.[75]

4.1.2.2. Serial dilution in droplets. Apart from the systems based on antibiotic printing, droplet-based systems are the most suitable systems for multiplexing AST and for being automated in general. The downside of such droplet-based AST is that flowing droplets do not support rapid AST. However, single-cell level (suggesting possible rapid AST) imaging in immobilized droplets has already been presented also with antibiotic multiplexing[121,122] – the drawback of these systems is that they are rather complicated, and each new antibiotic tested would require changes in the device design. A possible solution to this issue is repurposing the already existing platform for multiplexed AST in trapped droplets[53] for single-cell analysis – this would, however, require the preparation of all antibiotic solutions in a BioRad's QX200 cartridge (similar to a well plate) before the experiment which is impractical and on a large scale would require a specialized diagnostics laboratory. We suggest that in terms of multiplexing microfluidic ASTs, it would be best to pair a droplet-based dilution systems with a hybrid droplet-chamber array.

4.1.2.2.1. Microfluidic dilution systems. Automated microfluidic devices for the generation of concentration gradients are plentiful,[185] and some of the AST systems described in this manuscript contain such a generator. We are not going to describe in detail all such systems. Rather, we will briefly outline the challenges for the main classes of concentration gradient generators (dilutors) that are used or

could be used in droplet microfluidic AST. These main classes are i) diffusion-based dilutors;[186] ii) dilutors based on a coalescence of flowing droplets;[138] iii) dilutors based on trapped droplets.[130] The diffusion-based dilutors rely on the passive mixing of fluids flowing in microchannels before the droplet generation, the fluids in AST being an antibiotic stock solution, an antibiotic-free medium, and a bacterial sample. The main challenge in this kind of devices is the limited range of concentrations they can produce and limited multiplexing capabilities due to the large channel networks necessary for the systems to operate. A diffusion-based method that overcomes these issues was presented by Miller et al.[187] where the authors inject a portion of the drug (for ASTs, it would be an antibiotic), and the gradient is being generated through Taylor–Arys dispersion before droplet generation. This device was shown to operate at 3 orders of magnitude of drug concentrations, which is still not ideal for medical diagnostics. The droplet dilutors based on the coalescence of flowing droplets also suffer from a limited dynamic range: a droplet-based system for AST in droplets presented by Churski et al. contained a dilutor in which droplets of antibiotic and droplets of pure medium were coalesced in series.[138] Each coalescence event comprised droplets of different volume so that the ratio of antibiotic to pure medium droplet sizes was different each time, but the final merged droplet was always the same size. This heavily limits the dynamic range of the method as to cover a wide range of concentrations, an impractically small droplet would have to be merged with an impractically large droplet to achieve a highly diluted sample – Churski et al. report only two orders of magnitude dynamic range, similarly to a more recent integrated dilutor-AST system by Osaid et al.[74] Trap-based droplet dilutors offer, in theory, an infinite dynamic range of concentrations, as a trapped droplet can be diluted by subsequent diluent droplets indefinitely.[188] However, trap-based dilutors require stable flow of droplets to operate properly, as mixing in droplets during dilution depends on the flow rates of liquids in a dilution system.[189] There are reports, however, of successful integration of trap-based dilutors with droplet arrays[190,191] and also running AST in such devices.[124] Considering dilution errors, trap-based dilutors cumulate these errors: if the dilutions are done with 5% precision each, then the 10th dilution would have a concentration error of 50%, while dilutors as presented by Churski et al. generate sample concentrations with the same error for every dilution.

4.1.3. Inoculum effect considerations. Analysis of antibiotic susceptibility both in bulk and in microfluidics is haunted by the inoculum effect (IE). IE is the dependency of the measured MIC on the initial bacterial density[192,193] – once thought to be an artifact of the AST methods for β-lactam antibiotics with little to no clinical consequence.[194] Recently IE was demonstrated as a possible source of errors in assessing MIC according to Eucast and CLSI protocols.[86,88] CLSI requires a standardized inoculum density of 5×10^5 CFU ml^{-1} (CFU – colony-forming units, i.e., individual

bacterial cells) with an allowable range of 2×10^5 CFU ml^{-1} to 8×10^5 CFU ml^{-1}.[195] Smith and Kirby showed that operating AST within these allowed boundaries may already lead to a false MIC or breakpoint analysis.[86] IE was also registered in droplet-based systems,[130] and this raises concerns as to how to determine the bacteria concentrations on a microscale. AST seems not to be affected by the inoculum effect when the concentration of bacteria in the sample is so small that the bacteria are grown in their individual compartments, entirely or almost completely separated from other bacteria.[87,88,130] This robustness of AST for separated cells suggests that MIC measured for such compartmentalized bacteria, scMIC (single-cell minimum inhibitory concentration), is less prone to errors stemming from IE than the classical MIC measurements. As IE might be a challenge for AST measurements, microfluidics seems to be a possible answer to this problem: compartmentalization of individual bacteria in droplets or chambers might eliminate the problem of IE in AST. However, a new issue of merging scMIC data with the classically acquired MIC data arises: a CLSI-recommended 5×10^5 CFU ml^{-1} concentration of bacteria is identical to a concentration of one single bacterial cell (1 CFU) trapped in a 2 nl compartment. What will happen when a smaller or a larger compartment is used for AST? We have shown previously that the scMIC values are the same for the same bacterial strain and the same antibiotic (cefotaxime) in 740 pl and 2 nl droplets, albeit with different growth media. We could expect, however, that for very small compartments, scMIC would increase: in a smaller compartment, the number of antibiotic molecules per cell would be smaller. Therefore, the cell might survive higher concentrations of antibiotics. In such a case, it would perhaps be better to speak about MIA, the minimum inhibitory amount.[134] The increase in value of scMIC for very small compartments seems possible, as it was already demonstrated that quorum sensing was more pronounced in very small, 100 fl droplets than in bulk,[196] therefore a study of scMIC dependence on compartment volume would be welcome. Another problem with scMIC and IE in microfluidics is that when encapsulating individual cells, Poisson statistics apply[59] and even if the large majority of the compartments are empty, most of the bacteria-filled compartments contain exactly a single cell, still there are a fraction of compartments that contain two or more bacterial cells. We have already shown that there is a difference in measured MIC depending on whether there are 1, 2, 3, or more cells in a droplet,[130] so IE might be even more pronounced in droplets than in bulk due to large inoculum changes at such a small scale (inoculum difference between 1 and 2 cells is 100%, compare to a difference of 1% between 100 cells and 101 cells). The scMIC measurement is digital, however, so if from all the compartments that provide for bacterial growth, only 10% of compartments contained 2 or more cells at the beginning of the experiment, the false positive signal would only come from 10% compartments of interest. We predict that a proper statistical analysis could

account for this problem: if one knows the number of compartments that contained any cells in a population of compartments, one can calculate how many compartments in this experiment contain 2 or more cells at the beginning of the experiment and exclude this number of compartments from the readout. Yet another concern is the fact that a clonal population of bacteria shows a range of individual scMIC levels,[134] and it is important to set a definition of scMIC measured, e.g., scMIC that stops the growth of 100% or 50% of isolated cells.

4.1.4. Commercialization. AST measuring devices must be easy to use to be attractive for clinicians. From a healthcare professional perspective, a perfect AST assay should require patient sample collection only, and further procedures should be done by someone else or by an automated system. Ideally, the personnel operating on the samples would not need to be skillful in e.g., microfluidics to run a microfluidics-based AST assay. From the approaches to AST described here, this ease-of-use is best represented by printing antibiotics to microfluidic chambers or lab-on-a-disc devices: such chambers with pre-printed drugs could be used as cartridges to which samples would be added with a pipette, and the AST readout would be performed in the physician's office quickly. Antibiotics are being printed and dried commercially to 96-well-plates, so new microfluidic AST assays should be compared to such well-plate-based solutions: although well-plates are compatible with robotic liquid handling systems, their throughput is limited to 96 reactions per plate (compare to a thousand reactions on a chip with pre-printed antibiotics[75]) and single-cell analysis in not viable in bulk wells as bacteria can swim in a large reaction volume and individual cells are virtually impossible to follow on a large scale. Pheno-molecular assays were shown to be the fastest ASTs from clinical samples to readouts,[167] however it is questionable if such an assay would be run by a physician: rather, a lab technician would work on the assay in a centralized hospital laboratory. Single-cell-tracking optical assays suffer from limited multiplexing and would require major improvements in this area to be useful in a clinical setting, and flowing-droplet-based phenotypic AST assays are not suitable for clinical diagnostics – mostly due to droplet stability issues, leakage of dyes and antibiotics between surfactant-stabilized droplets, and complexity in droplet preparation in comparison to microfluidic chambers.

4.2. Opportunities

The most clinically relevant application of microfluidics in antibiotics studies is AST. However, there are other antibiotic-related research paths that can be followed using microfluidic methods. Some of these possible research areas could be explored even with the existing technologies designed for ASTs or for other applications e.g., in analytical chemistry. Here, we highlight some of the most exciting and achievable antibiotic-related research topics available for microfluidics.

4.2.1. Rare events. Antibiotic heteroresistance is a phenotype in which the isogenic bacterial population contains a subpopulation of cells with reduced antibiotic susceptibility compared with the main population,[197] and it is attributed to antibiotic treatment failure for several bacteria species.[198–204] The variabilities in cells' response to the antibiotic can be attributed to genetic, epigenetic, and nongenetic mechanisms.[205] The main methods currently used to detect bacterial heteroresistance are PAP (population analysis profile) test, Etest, and disc diffusion.[205] In the PAP test, the bacterial population is cultured on the agar plates containing different antibiotic concentrations (usually 2-fold increments), and the grown colonies are counted at each of these concentrations. The PAP test is a gold standard and the most reliable method, but it is used only to confirm specific clinical cases due to its labor intensity and high costs. Broth microdilution, automated broth (for example, VITEK® 2), and growth methods (for example, BACTEC 960) are also used to detect heteroresistance, but they show low sensitivity, and the results can be affected by the inoculum effect.

New approaches to this problem take advantage of droplet microfluidics: Sun et al. presented a digital droplet PCR to detect resistance genes and point mutations in H. pylori cells in stool samples.[206] Scheler et al.[134] and Lyu et al.[133] demonstrated a digital quantification of the heteroresistance based on single-cell MIC determination. Techniques combining microfluidic devices with microscopy, where the growth of many individual cells is observed over time in the presence and absence of antibiotics[113] are promising as well. There is still room for improvement in microfluidic detection of heteroresistance, especially in multiplexing and in label-free readout.

4.2.2. Stochastic gene expression levels. We have recently shown that an isogenic population of bacteria contains cells that have different levels of individual antibiotic resistance, i.e., each cell has its own scMIC.[130,134] It would be interesting to see if a distribution of resistance levels in a population is caused by stochasticity in gene expression,[207] by the distribution of copy number of plasmids with resistance genes among a population, or a combination of both. Running a droplet-based scMIC assay on a strain of bacteria containing a resistance gene on a chromosome instead of a plasmid would eliminate the influence of plasmid copy number on individual resistance levels. Could scMIC distributions be manipulated with adjuvants or by adding other antibiotics to bacteria? A narrow scMIC distribution would be welcome in the clinic, as all the bacteria in the patient would be similarly easy (or similarly difficult) to eliminate. It would also be worthwhile to investigate the interactions of bacteria in the presence of antibiotics: is the resistance of two cells in a droplet a sum of the resistances of individual cells? Is there a difference in such interactions in droplets that are only slightly larger than bacterial cells?

4.2.3. Bacterial persistence. scMIC distribution is probably rooted in gene expression, while the non-genetic mechanisms are implicated in the formation of persister cells and, in

some cases, small colony variants (SCVs). Both survive the presence of a high antibiotic concentration but for a finite time of treatment.[208] They were found in several species and for several antibiotic classes, causing various infections from acute to chronic and recalcitrant.[209] The growth of SCVs is arrested, metabolism is reduced, they can colonize infected organs, be protected from the immune system, and therefore show higher tolerance towards antibiotics.[210,211] SCVs can alter the phenotype between non-growing and growing (susceptible to antibiotics), rendering the analysis and detection challenges.

The standard method for quantifying persister cells or small colony variants is a colony counting assay, which is a tedious and expensive approach.[212] Innovative microfluidic technology combines a mother machine with live-cell imaging, which allows for bacteria growth observation in various conditions.[104] It provides a sensitive analysis of the antibiotic susceptibility distribution of cells in the bacterial population. However, it produces a massive amount of data for analysis, making the application of this method difficult in clinical microbiology. High-throughput methods are required to detect persisting tolerant to antibiotics cells in the bacterial population as persisters are rare, and such an assay could benefit from the large scale of droplet microfluidics.

4.2.4. Evolution studies. There are several microfluidic assays that allow for observing the evolution of antibiotic resistance. The first system designed for this was called "death galaxy" by Austin *et al.* and comprised a set of interconnected microfluidic chambers to which antibiotics were introduced through diffusion through a series of slits that stopped bacteria from infecting the fresh media source.[44] Microdroplet chemostats were presented in different forms[126,127,213,214] that allowed for observation of antibiotic resistance changes in hundreds of separated bacteria populations in large microliter droplets – the media used by growing bacteria would be partially removed in an automated fashion, and portions of fresh media with a higher than before antibiotic concentration would be introduced instead. We believe that evolution studies would be improved if a microdroplet chemostat could operate on single cells, *i.e.*, after each exchange of the medium, a single cell would remain per droplet: this would allow for analysis of rates of emergence of resistance from a large number of clones and couple with the research of individual bacteria scMIC would inform about whether clonally identical but more resistant cells gain resistance faster than their isogenic yet less resistant counterparts. We think that droplet microfluidics is particularly well developed for such a goal; however, an array of chambers with each chamber controlled *via* a valve could also be a viable option. A part of this research vision was presented in large droplets, where bacterial growth in 1000 oscillating droplets of which some contained single cells, was followed over 13 hours,[215] although the used device was not a chemostat: there was no addition of fresh medium to the oscillating droplets.

Additionally, the chosen average number of cells per droplet (λ in the Poisson distribution) of 0.5 meant that 25% of all droplets containing bacteria contained more than one cell at the beginning of the experiment, and fluorescence levels of cells were used as a proxy for fitness – direct scMIC measurements would be more informative.

Measurements of metabolism level of bacteria in droplets[156] were recently used for microfluidic AST based on analysis of metabolism levels of cells as a phenotype.[144,145] Such methods could be further developed to, *e.g.*, sort out cells with high metabolism rates and identify their rates of emergence of antibiotic resistance with a single-cell microchemostat we propose in the previous paragraph. Is a higher metabolism level correlated with a higher rate of resistance emergence?

4.2.5. Biofilm studies. Microfluidic techniques have been used to analyze the emergence of biofilms,[216] also in droplets – perhaps not intuitively, biofilms can form on the inner surface of a droplet.[217] A microfluidic assay in which different parts of a biofilm were automatically sampled at a time interval and the collected cells analyzed for scMIC could be highly informative about the dynamics of antibiotic resistance of an aging biofilm at a single-cell level. Are the cells of the same age in a biofilm equally resistant? Perhaps there are subpopulations of highly resistant cells? Or is there a resistance distribution in a biofilm's equally old cells as in a population of swimming bacteria?

5. Concluding remarks

Antibiotic susceptibility testing research has gained considerable momentum thanks to microfluidic technologies. A wide variety of approaches to the AST field, such as single-cell optical tracking, sampling bacteria to chambers pre-filled with antibiotics, complex droplet-based systems, or pheno-molecular microfluidic assays, show the robustness of microfluidics in microbiology. The AST sample-to-detection time is already superb in some microfluidic assays and now it is mostly multiplexing of different antibiotics and different antibiotic concentrations that needs to be added on top of short assay times that is a technological bottleneck for microfluidic AST. If this bottleneck is overcome, then most requirements for an ideal AST assay would be achieved. The problem that will remain unchanged is the fact that the largest market for AST platforms is the US and EU,[218] while the regions with the largest antibiotic-resistance-related problems in the world are Africa and Asia. Although the road to a highly informative multiplexed and fast microfluidic AST assay with the clinical application is not long, the challenge that looms on the horizon lies in introducing such a platform to countries that suffer the most from infectious diseases.

Conflicts of interest

There are no conflicts to declare.

Acknowledgements

References

1 A. Fleming, Nobel Prize.

2 C. L. Ventola, *Pharmacol. Ther.*, 2015, **40**, 277–283.

3 ECDC/EMEA, The bacterial challenge: time to react, 2009.

4 CDC, Antibiotic Resistance Threats in the United States, 2019, 2019.

5 N. Daulaire, A. Bang, G. Tomson, J. N. Kalyango and O. Cars, *J. Law Med. Ethics*, 2015, **43**, 17–21.

6 M. E. A. de Kraker, A. J. Stewardson and S. Harbarth, *PLoS Med.*, 2016, **13**, e1002184.

7 C. Abbafati, K. M. Abbas, M. Abbasi-Kangevari, F. Abd-Allah, A. Abdelalim, M. Abdollahi, I. Abdollahpour, K. H. Abegaz, H. Abolhassani, V. Aboyans, L. G. Abreu, M. R. M. Abrigo, A. Abualhasan, L. J. Abu-Raddad, A. I. Abushouk, M. Adabi, V. Adekanmbi, A. M. Adeoye, O. O. Adetokunboh, D. Adham, S. M. Advani, A. Afshin, G. Agarwal, S. M. K. Aghamir, A. Agrawal, T. Ahmad, K. Ahmadi, M. Ahmadi, H. Ahmadieh, M. B. Ahmed, T. Y. Akalu, R. O. Akinyemi, T. Akinyemiju, B. Akombi, C. J. Akunna, F. Alahdab, Z. Al-Aly, K. Alam, S. Alam, T. Alam, F. M. Alanezi, T. M. Alanzi, B. W. Alemu, K. F. Alhabib, M. Ali, S. Ali, G. Alicandro, C. Alinia, V. Alipour, H. Alizade, S. M. Aljunid, F. Alla, P. Allebeck, A. Almasi-Hashiani, H. M. Al-Mekhlafi, J. Alonso, K. A. Altirkawi, M. Amini-Rarani, F. Amiri, D. A. Amugsi, R. Ancuceanu, D. Anderlini, J. A. Anderson, C. L. Andrei, T. Andrei, C. Angus, M. Anjomshoa, F. Ansari, A. Ansari-Moghaddam, I. C. Antonazzo, C. A. T. Antonio, C. M. Antony, E. Antriyandarti, D. Anvari, R. Anwer, S. C. Y. Appiah, J. Arabloo, M. Arab-Zozani, A. Y. Aravkin, F. Ariani, B. Armoon, J. Ärnlöv, A. Arzani, M. Asadi-Aliabadi, A. A. Asadi-Pooya, C. Ashbaugh, M. Assmus, Z. Atafar, D. D. Atnafu, M. M. D. W. Atout, F. Ausloos, M. Ausloos, B. P. Ayala Quintanilla, G. Ayano, M. A. Ayanore, S. Azari, G. Azarian, Z. N. Azene, A. Badawi, A. D. Badiye, M. A. Bahrami, M. H. Bakhshaei, A. Bakhtiari, S. M. Bakkannavar, A. Baldasseroni, K. Ball, S. H. Ballew, D. Balzi, M. Banach, S. K. Banerjee, A. B. Bante, A. G. Baraki, S. L. Barker-Collo, T. W. Bärnighausen, L. H. Barrero, C. M. Barthelemy, L. Barua, S. Basu, B. T. Baune, M. Bayati, J. S. Becker, N. Bedi, E. Beghi, Y. Béjot, M. L. Bell, F. B. Bennitt, I. M. Bensenor, K. Berhe, A. E. Berman, A. S. Bhagavathula, R. Bhageerathy, N. Bhala, D. Bhandari, K. Bhattacharyya, Z. A. Bhutta, A. Bijani, B. Bikbov, M. S. Bin Sayeed, A. Biondi, B. M. Birihane, C. Bisignano, R. K. Biswas, H. Bitew, S. Bohlouli, M. Bohluli, A. S. Boon-Dooley, G. Borges, A. M. Borzì, S. Borzouei, C. Bosetti, S. Boufous, D. Braithwaite, M. Brauer, N. J. K. Breitborde, S. Breitner, H. Brenner, P. S. Briant, A. N. Briko, N. I. Briko, G. B. Britton, D. Bryazka, B. R. Bumgarner, K. Burkart, R. T. Burnett, S. Burugina Nagaraja, Z. A. Butt, F. L. Caetano Dos Santos, L. E. Cahill, L. A. Cámera, I. R. Campos-Nonato, R. Cárdenas, G. Carreras, J. J. Carrero, F. Carvalho, J. M. Castaldelli-Maia, C. A. Castañeda-Orjuela, G. Castelpietra, F. Castro, K. Causey, C. R. Cederroth, K. M. Cercy, E. Cerin, J. S. Chandan, K. L. Chang, F. J. Charlson, V. K. Chattu, S. Chaturvedi, N. Cherbuin, O. Chimed-Ochir, D. Y. Cho, J. Y. J. Choi, H. Christensen, D. T. Chu, M. T. Chung, S. C. Chung, F. M. Cicuttini, L. G. Ciobanu, M. Cirillo, T. K. D. Classen, A. J. Cohen, K. Compton, O. R. Cooper, V. M. Costa, E. Cousin, R. G. Cowden, D. H. Cross, J. A. Cruz, S. M. A. Dahlawi, A. A. M. Damasceno, G. Damiani, L. Dandona, R. Dandona, W. J. Dangel, A. K. Danielsson, P. I. Dargan, A. M. Darwesh, A. Daryani, J. K. Das, R. Das Gupta, J. das Neves, C. A. Dávila-Cervantes, D. V. Davitoiu, D. De Leo, L. Degenhardt, M. DeLang, R. P. Dellavalle, F. M. Demeke, G. T. Demoz, D. G. Demsie, E. Denova-Gutiérrez, N. Dervenis, G. P. Dhungana, M. Dianatinasab, D. Dias da Silva, D. Diaz, Z. S. Dibaji Forooshani, S. Djalalinia, H. T. Do, K. Dokova, F. Dorostkar, L. Doshmangir, T. R. Driscoll, B. B. Duncan, A. R. Duraes, A. W. Eagan, D. Edvardsson, N. El Nahas, I. El Sayed, M. El Tantawi, I. Elbarazi, I. Y. Elgendy, S. I. El-Jaafary, I. R. F. Elyazar, S. Emmons-Bell, H. E. Erskine, S. Eskandarieh, S. Esmaeilnejad, A. Esteghamati, K. Estep, A. Etemadi, A. E. Etisso, J. Fanzo, M. Farahmand, M. Fareed, R. Faridnia, A. Farioli, A. Faro, M. Faruque, F. Farzadfar, N. Fattahi, M. Fazlzadeh, V. L. Feigin, R. Feldman, S. M. Fereshtehnejad, E. Fernandes, G. Ferrara, A. J. Ferrari, M. L. Ferreira, I. Filip, F. Fischer, J. L. Fisher, L. S. Flor, N. A. Foigt, M. O. Folayan, A. A. Fomenkov, L. M. Force, M. Foroutan, R. C. Franklin, M. Freitas, W. Fu, T. Fukumoto, J. M. Furtado, M. M. Gad, E. Gakidou, S. Gallus, A. L. Garcia-Basteiro, W. M. Gardner, B. S. Geberemariyam, A. A. A. Ayalew Gebreslassie, A. Geremew, A. Gershberg Hayoon, P. W. Gething, M. Ghadimi, K. Ghadiri, F. Ghaffarifar, M. Ghafourifard, F. Ghamari, A. Ghashghaee, H. Ghiasvand, N. Ghith, A. Gholamian, R. Ghosh, P. S. Gill, T. G. Ginindza, G. Giussani, E. V. Gnedovskaya, S. Goharinezhad, S. V. Gopalani, G. Gorini, H. Goudarzi, A. C. Goulart, F. Greaves, M. Grivna, G. Grosso, M. I. M. Gubari, H. C. Gugnani, R. A. Guimarães, R. A. Guled, G. Guo, Y. Guo, R. Gupta, T. Gupta, B. Haddock, N. Hafezi-Nejad, A. Hafiz, A. Haj-Mirzaian, A. Haj-Mirzaian, B. J. Hall, I. Halvaei, R. R. Hamadeh, S. Hamidi, M. S. Hammer, G. J. Hankey, H. Haririan, J. M. Haro, A. I. Hasaballah, M. M. Hasan, E. Hasanpoor, A. Hashi, S. Hassanipour, H. Hassankhani, R. J. Havmoeller, S. I. Hay, K. Hayat, G. Heidari, R. Heidari-Soureshjani, H. J. Henrikson, M. E. Herbert, C. Herteliu, F. Heydarpour, T. R. Hird, H. W. Hoek, R. Holla, P. Hoogar, H. D. Hosgood, N. Hossain, M. Hosseini, M. Hosseinzadeh, M. Hostiuc, S. Hostiuc, M. Househ, M. Hsairi, V. C. R. Hsieh, G. Hu, K.

Hu, T. M. Huda, A. Humayun, C. K. Huynh, B. F. Hwang, V. C. Iannucci, S. E. Ibitoye, N. Ikeda, K. S. Ikuta, O. S. Ilesanmi, I. M. Ilic, M. D. Ilic, L. R. Inbaraj, H. Ippolito, U. Iqbal, S. S. N. Irvani, C. M. S. Irvine, M. M. Islam, S. M. S. Islam, H. Iso, R. Q. Ivers, C. C. D. Iwu, C. J. Iwu, I. O. Iyamu, J. Jaafari, K. H. Jacobsen, H. Jafari, M. Jafarinia, M. A. Jahani, M. Jakovljevic, F. Jalilian, S. L. James, H. Janjani, T. Javaheri, J. Javidnia, P. Jeemon, E. Jenabi, R. P. Jha, V. Jha, J. S. Ji, L. Johansson, O. John, Y. O. John-Akinola, C. O. Johnson, J. B. Jonas, F. Joukar, J. J. Jozwiak, M. Jürisson, A. Kabir, Z. Kabir, H. Kalani, R. Kalani, L. R. Kalankesh, R. Kalhor, T. Kanchan, N. Kapoor, B. K. Matin, A. Karch, M. A. Karim, G. M. Kassa, S. V. Katikireddi, G. A. Kayode, A. Kazemi Karyani, P. N. Keiyoro, C. Keller, L. Kemmer, P. J. Kendrick, N. Khalid, M. Khammarnia, E. A. Khan, M. Khan, K. Khatab, M. M. Khater, M. N. Khatib, M. Khayamzadeh, S. Khazaei, C. Kieling, Y. J. Kim, R. W. Kimokoti, A. Kisa, S. Kisa, M. Kivimäki, L. D. Knibbs, A. K. S. Knudsen, J. M. Kocarnik, S. Kochhar, J. A. Kopec, V. A. Korshunov, P. A. Koul, A. Koyanagi, M. U. G. Kraemer, K. Krishan, K. J. Krohn, H. Kromhout, B. Kuate Defo, G. A. Kumar, V. Kumar, O. P. Kurmi, D. Kusuma, C. La Vecchia, B. Lacey, D. K. Lal, R. Lalloo, T. Lallukka, F. H. Lami, I. Landires, J. J. Lang, S. M. Langan, A. O. Larsson, S. Lasrado, P. Lauriola, J. V. Lazarus, P. H. Lee, S. W. H. Lee, K. E. Legrand, J. Leigh, M. Leonardi, H. Lescinsky, J. Leung, M. Levi, S. Li, L. L. Lim, S. Linn, S. Liu, S. Liu, Y. Liu, J. Lo, A. D. Lopez, J. C. F. Lopez, P. D. Lopukhov, S. Lorkowski, P. A. Lotufo, A. Lu, A. Lugo, E. R. Maddison, P. W. Mahasha, M. M. Mahdavi, M. Mahmoudi, A. Majeed, A. Maleki, S. Maleki, R. Malekzadeh, D. C. Malta, A. A. Mamun, A. L. Manda, H. Manguerra, F. Mansour-Ghanaei, B. Mansouri, M. A. Mansournia, A. M. Mantilla Herrera, J. C. Maravilla, A. Marks, R. V. Martin, S. Martini, F. R. Martins-Melo, A. Masaka, S. Z. Masoumi, M. R. Mathur, K. Matsushita, P. K. Maulik, C. McAlinden, J. J. McGrath, M. McKee, M. M. Mehndiratta, F. Mehri, K. M. Mehta, Z. A. Memish, W. Mendoza, R. G. Menezes, E. W. Mengesha, A. Mereke, S. T. Mereta, A. Meretoja, T. J. Meretoja, T. Mestrovic, B. Miazgowski, T. Miazgowski, I. M. Michalek, T. R. Miller, E. J. Mills, G. K. Mini, M. Miri, A. Mirica, E. M. Mirrakhimov, H. Mirzaei, M. Mirzaei, R. Mirzaei, M. Mirzaei-Alavijeh, A. T. Misganaw, P. Mithra, B. Moazen, D. K. Mohammad, Y. Mohammad, N. Mohammad Gholi Mezerji, A. Mohammadian-Hafshejani, N. Mohammadifard, R. Mohammadpourhodki, A. S. Mohammed, H. Mohammed, J. A. Mohammed, S. Mohammed, A. H. Mokdad, M. Molokhia, L. Monasta, M. D. Mooney, G. Moradi, M. Moradi, M. Moradi-Lakeh, R. Moradzadeh, P. Moraga, L. Morawska, J. Morgado-Da-Costa, S. D. Morrison, A. Mosapour, J. F. Mosser, S. Mouodi, S. M. Mousavi, A. M. Khaneghah, U. O. Mueller, S. Mukhopadhyay, E. C. Mullany, K. I. Musa, S. Muthupandian, A. F. Nabhan, M. Naderi, A. J. Nagarajan, G. Nagel, M. Naghavi, B. Naghshtabrizi, M. D. Naimzada, F. Najafi, V. Nangia, J. R. Nansseu, M. Naserbakht, V. C. Nayak, I. Negoi, J. W.

Ngunjiri, C. T. Nguyen, H. L. T. Nguyen, M. Nguyen, Y. T. Nigatu, R. Nikbakhsh, M. R. Nixon, C. A. Nnaji, S. Nomura, B. Norrving, J. J. Noubiap, C. Nowak, V. Nunez-Samudio, B. Oancea, C. M. Odell, F. A. Ogbo, I. H. Oh, E. W. Okunga, M. Oladnabi, A. T. Olagunju, B. O. Olusanya, J. O. Olusanya, M. O. Omer, K. L. Ong, O. E. Onwujekwe, H. M. Orpana, A. Ortiz, O. Osarenotor, F. B. Osei, S. M. Ostroff, A. Otoiu, N. Otstavnov, S. S. Otstavnov, S. Øverland, M. O. Owolabi, P. A. Mahesh, J. R. Padubidri, R. Palladino, S. Panda-Jonas, A. Pandey, C. D. H. Parry, M. Pasovic, D. K. Pasupula, S. K. Patel, M. Pathak, S. B. Patten, G. C. Patton, H. P. Toroudi, A. E. Peden, A. Pennini, V. C. F. Pepito, E. K. Peprah, D. M. Pereira, K. Pesudovs, H. Q. Pham, M. R. Phillips, C. Piccinelli, T. M. Pilz, M. A. Piradov, M. Pirsaheb, D. Plass, S. Polinder, K. R. Polkinghorne, C. D. Pond, M. J. Postma, H. Pourjafar, F. Pourmalek, A. Poznañska, S. I. Prada, V. Prakash, D. R. A. Pribadi, E. Pupillo, Z. Q. Syed, M. Rabiee, N. Rabiee, A. Radfar, A. Rafiee, A. Raggi, M. A. Rahman, A. Rajabpour-Sanati, F. Rajati, I. Rakovac, P. Ram, K. Ramezanzadeh, C. L. Ranabhat, P. C. Rao, S. J. Rao, V. Rashedi, P. Rathi, D. L. Rawaf, S. Rawaf, L. Rawal, R. Rawassizadeh, R. Rawat, C. Razo, S. B. Redford, R. C. Reiner, M. B. Reitsma, G. Remuzzi, V. Renjith, A. M. N. Renzaho, S. Resnikoff, N. Rezaei, N. Rezaei, A. Rezapour, P. A. Rhinehart, S. M. Riahi, D. C. Ribeiro, D. Ribeiro, J. Rickard, J. A. Rivera, N. L. S. Roberts, S. Rodríguez-Ramírez, L. Roever, L. Ronfani, R. Room, G. Roshandel, G. A. Roth, D. Rothenbacher, E. Rubagotti, G. M. Rwegerera, S. Sabour, P. S. Sachdev, B. Saddik, E. Sadeghi, M. Sadeghi, R. Saeedi, S. Saeedi Moghaddam, Y. Safari, S. Safi, S. Safiri, R. Sagar, A. Sahebkar, S. M. Sajadi, N. Salam, P. Salamati, H. Salem, M. R. Salem, H. Salimzadeh, O. M. Salman, J. A. Salomon, Z. Samad, H. Samadi Kafil, E. Z. Sambala, A. M. Samy, J. Sanabria, T. G. Sánchez-Pimienta, D. F. Santomauro, I. S. Santos, J. V. Santos, M. M. Santric-Milicevic, S. Y. I. Saraswathy, R. Sarmiento-Suárez, N. Sarrafzadegan, B. Sartorius, A. Sarveazad, B. Sathian, T. Sathish, D. Sattin, S. Saxena, L. E. Schaeffer, S. Schiavolin, M. P. Schlaich, M. I. Schmidt, A. E. Schutte, D. C. Schwebel, F. Schwendicke, A. M. Senbeta, S. Senthilkumaran, S. G. Sepanlou, B. Serdar, M. L. Serre, O. Shafaat, S. Shahabi, A. A. Shaheen, M. A. Shaikh, A. S. Shalash, M. Shams-Beyranvand, M. Shamsizadeh, K. Sharafi, A. Sheikh, A. Sheikhtaheri, K. Shibuya, K. D. Shield, M. Shigematsu, J. Il Shin, M. J. Shin, R. Shiri, R. Shirkoohi, K. Shuval, S. Siabani, R. Sierpinski, I. D. Sigfusdottir, R. Sigurvinsdottir, J. P. Silva, K. E. Simpson, J. A. Singh, P. Singh, E. Skiadaresi, S. T. Skou, V. Y. Skryabin, E. U. R. Smith, A. Soheili, S. Soltani, M. Soofi, R. J. D. Sorensen, J. B. Soriano, M. B. Sorrie, S. Soshnikov, I. N. Soyiri, C. N. Spencer, A. Spotin, C. T. Sreeramareddy, V. Srinivasan, J. D. Stanaway, C. Stein, D. J. Stein, C. Steiner, L. Stockfelt, M. A. Stokes, K. Straif, J. L. Stubbs, M. B. Sufiyan, H. A. R. Suleria, R. Suliankatchi Abdulkader, G. Sulo, I. Sultan, R. Tabarés-Seisdedos, K. M. Tabb, T. Tabuchi, A. Taherkhani, M. Tajdini, K. Takahashi, J. S. Takala, A. T. Tamiru, N. Taveira,

A. Tehrani-Banihashemi, M. H. Temsah, G. A. Tesema, Z. T. Tessema, G. D. Thurston, M. V. Titova, H. R. Tohidinik, M. Tonelli, R. Topor-Madry, F. Topouzis, A. E. Torre, M. Touvier, M. R. Tovani-Palone, B. X. Tran, R. Travillian, A. Tsatsakis, L. T. Tudor Car, S. Tyrovolas, R. Uddin, C. D. Umeokonkwo, B. Unnikrishnan, E. Upadhyay, M. Vacante, P. R. Valdez, A. van Donkelaar, T. J. Vasankari, Y. Vasseghian, Y. Veisani, N. Venketasubramanian, F. S. Violante, V. Vlassov, S. E. Vollset, T. Vos, R. Vukovic, Y. Waheed, M. T. Wallin, Y. Wang, Y. P. Wang, A. Watson, J. Wei, M. Y. W. Wei, R. G. Weintraub, J. Weiss, A. Werdecker, J. J. West, R. Westerman, J. L. Whisnant, H. A. Whiteford, K. E. Wiens, C. D. A. Wolfe, S. S. Wozniak, A. M. Wu, J. Wu, S. Wulf Hanson, G. Xu, R. Xu, S. Yadgir, S. H. Yahyazadeh Jabbari, K. Yamagishi, M. Yaminfirooz, Y. Yano, S. Yaya, V. Yazdi-Feyzabadi, T. Y. Yeheyis, C. S. Yilgwan, M. T. Yilma, P. Yip, N. Yonemoto, M. Z. Younis, T. P. Younker, B. Yousefi, Z. Yousefi, T. Yousefinezhadi, A. Y. Yousuf, C. Yu, H. Yusefzadeh, T. Z. Moghadam, M. Zamani, M. Zamanian, H. Zandian, M. S. Zastrozhin, Y. Zhang, Z. J. Zhang, J. T. Zhao, X. J. G. Zhao, Y. Zhao, P. Zheng, M. Zhou, K. Davletov, A. Ziapour, S. Mondello, S. S. Lim, C. J. L. Murray, T. Wiangkham and S. Amini, *Lancet*, 2020, **396**, 1204–1222.

8 C. J. Murray, K. S. Ikuta, F. Sharara, L. Swetschinski, G. Robles Aguilar, A. Gray, C. Han, C. Bisignano, P. Rao, E. Wool, S. C. Johnson, A. J. Browne, M. G. Chipeta, F. Fell, S. Hackett, G. Haines-Woodhouse, B. H. Kashef Hamadani, E. A. P. Kumaran, B. McManigal, R. Agarwal, S. Akech, S. Albertson, J. Amuasi, J. Andrews, A. Aravkin, E. Ashley, F. Bailey, S. Baker, B. Basnyat, A. Bekker, R. Bender, A. Bethou, J. Bielicki, S. Boonkasidecha, J. Bukosia, C. Carvalheiro, C. Castañeda-Orjuela, V. Chansamouth, S. Chaurasia, S. Chiurchiù, F. Chowdhury, A. J. Cook, B. Cooper, T. R. Cressey, E. Criollo-Mora, M. Cunningham, S. Darboe, N. P. J. Day, M. De Luca, K. Dokova, A. Dramowski, S. J. Dunachie, T. Eckmanns, D. Eibach, A. Emami, N. Feasey, N. Fisher-Pearson, K. Forrest, D. Garrett, P. Gastmeier, A. Z. Giref, R. C. Greer, V. Gupta, S. Haller, A. Haselbeck, S. I. Hay, M. Holm, S. Hopkins, K. C. Iregbu, J. Jacobs, D. Jarovsky, F. Javanmardi, M. Khorana, N. Kissoon, E. Kobeissi, T. Kostyanev, F. Krapp, R. Krumkamp, A. Kumar, H. H. Kyu, C. Lim, D. Limmathurotsakul, M. J. Loftus, M. Lunn, J. Ma, N. Mturi, T. Munera-Huertas, P. Musicha, M. M. Mussi-Pinhata, T. Nakamura, R. Nanavati, S. Nangia, P. Newton, C. Ngoun, A. Novotney, D. Nwakanma, C. W. Obiero, A. Olivas-Martinez, P. Olliaro, E. Ooko, E. Ortiz-Brizuela, A. Y. Peleg, C. Perrone, N. Plakkal, A. Ponce-de-Leon, M. Raad, T. Ramdin, A. Riddell, T. Roberts, J. V. Robotham, A. Roca, K. E. Rudd, N. Russell, J. Schnall, J. A. G. Scott, M. Shivamallappa, J. Sifuentes-Osornio, N. Steenkeste, A. J. Stewardson, T. Stoeva, N. Tasak, A. Thaiprakong, G. Thwaites, C. Turner, P. Turner, H. R. van Doorn, S. Velaphi, A. Vongpradith, H. Vu, T. Walsh, S. Waner, T. Wangrangsimakul, T. Wozniak, P. Zheng, B. Sartorius, A. D. Lopez, A. Stergachis, C. Moore, C. Dolecek and M. Naghavi, *Lancet*, 2022, **399**, 629–655.

9 J. O'Neill, *Tackling Drug-Resistant Infections Globally: Final Report And Recommendations*, 2016.

10 H. Nikaido, *Annu. Rev. Biochem.*, 2009, **78**, 119–146.

11 K. M. G. O'Connell, J. T. Hodgkinson, H. F. Sore, M. Welch, G. P. C. Salmond and D. R. Spring, *Angew. Chem., Int. Ed.*, 2013, **52**, 10706–10733.

12 C.-E. Luyt, N. Bréchot, J.-L. Trouillet and J. Chastre, *Crit. Care*, 2014, **18**, 480.

13 C. Casals-Pascual, A. Vergara and J. Vila, *Hum. Microbiome J.*, 2018, **9**, 11–15.

14 D. G. J. Larsson and C. F. Flach, *Nat. Rev. Microbiol.*, 2021, **20**(5), 257–269.

15 T. Buschhardt, T. Günther, T. Skjerdal, M. Torpdahl, J. Gethmann, M. E. Filippitzi, C. Maassen, S. Jore, J. Ellis-Iversen and M. Filter, *One Health*, 2021, **13**, 100263.

16 G. Worrall, J. Hutchinson, G. Sherman and J. Griffiths, *Can. Fam. Physician*, 2007, **53**, 666–671.

17 J.-P. Humair, S. A. Revaz, P. Bovier and H. Stalder, *Arch. Intern. Med.*, 2006, **166**, 640.

18 W. J. McIsaac, J. D. Kellner, P. Aufricht, A. Vanjaka and D. E. Low, *JAMA*, 2004, **291**, 1587.

19 J. M. Andrews, *J. Antimicrob. Chemother.*, 2001, **48**, 5–16.

20 G. Kahlmeter, D. F. J. Brown, F. W. Goldstein, A. P. MacGowan, J. W. Mouton, A. Österlund, A. Rodloff, M. Steinbakk, P. Urbaskova and A. Vatopoulos, *J. Antimicrob. Chemother.*, 2003, **52**, 145–148.

21 J. Turnidge and D. L. Paterson, *Clin. Microbiol. Rev.*, 2007, **20**, 391–408.

22 D. L. Paterson, W.-C. Ko, A. Von Gottberg, J. M. Casellas, L. Mulazimoglu, K. P. Klugman, R. A. Bonomo, L. B. Rice, J. G. McCormack and V. L. Yu, *J. Clin. Microbiol.*, 2001, **39**, 2206–2212.

23 J. Cama, R. Leszczynski, P. K. Tang, A. Khalid, V. Lok, C. G. Dowson and A. Ebata, *ACS Infect. Dis.*, 2021, **7**, 2029–2042.

24 I. A. Dutescu and S. A. Hillie, *Infect. Drug Resist.*, 2021, **14**, 415–434.

25 A. Mullard, *Nat. Rev. Drug Discovery*, 2022, **21**, 406.

26 M. J. Renwick, D. M. Brogan and E. Mossialos, *J. Antibiot.*, 2016, **69**, 73–88.

27 A. van Belkum, C. A. D. Burnham, J. W. A. Rossen, F. Mallard, O. Rochas and W. M. Dunne, *Nat. Rev. Microbiol.*, 2020, **18**, 299–311.

28 K. Zhang, S. Qin, S. Wu, Y. Liang and J. Li, *Chem. Sci.*, 2020, **11**, 6352–6361.

29 N. Qin, P. Zhao, E. A. Ho, G. Xin and C. L. Ren, *ACS Sens.*, 2021, **6**, 3–21.

30 A. Vasala, V. P. Hytönen and O. H. Laitinen, *Front. Cell. Infect. Microbiol.*, 2020, **10**, 308.

31 Z. A. Khan, M. F. Siddiqui and S. Park, *Diagnostics*, 2019, **9**, 49.

32 A. van Belkum, T. T. Bachmann, G. Lüdke, J. G. Lisby, G. Kahlmeter, A. Mohess, K. Becker, J. P. Hays, N. Woodford, K. Mitsakakis, J. Moran-Gilad, J. Vila, H. Peter, J. H. Rex and W. M. Dunne, *Nat. Rev. Microbiol.*, 2018, **17**(1), 51–62.

33 Y. Xia and G. M. Whitesides, *Annu. Rev. Mater. Sci.*, 1998, **28**, 153–184.

34 D. J. Guckenberger, T. E. de Groot, A. M. D. Wan, D. J. Beebe and E. W. K. Young, *Lab Chip*, 2015, **15**, 2364–2378.

35 J. M. K. Ng, I. Gitlin, A. D. Stroock and G. M. Whitesides, *Electrophoresis*, 2002, **23**, 3461–3473.

36 K. M. Raj and S. Chakraborty, *J. Appl. Polym. Sci.*, 2020, **137**, 48958.

37 B. Gale, A. Jafek, C. Lambert, B. Goenner, H. Moghimifam, U. Nze and S. Kamarapu, *Inventions*, 2018, **3**, 60.

38 P. Zhu and L. Wang, *Lab Chip*, 2017, **17**, 34–75.

39 S. L. Anna, *Annu. Rev. Fluid Mech.*, 2016, **48**, 285–309.

40 S. K. W. Dertinger, D. T. Chiu, N. L. Jeon and G. M. Whitesides, *Anal. Chem.*, 2001, **73**, 1240–1246.

41 M. A. Unger, H.-P. Chou, T. Thorsen, A. Scherer and S. R. Quake, *Science*, 2000, **288**, 113–116.

42 D. S. Liao, J. Raveendran, S. Golchi and A. Docoslis, *Sens. Bio-Sens. Res.*, 2015, **6**, 59–66.

43 Q. Zhu, L. Qiu, B. Yu, Y. Xu, Y. Gao, T. Pan, Q. Tian, Q. Song, W. Jin, Q. Jin and Y. Mu, *Lab Chip*, 2014, **14**, 1176–1185.

44 R. H. A. Q. Zhang, G. Lambert, D. Liao, H. Kim, K. Robin, C.-k. Tung, N. Pourmand and R. H. Austin, *Science*, 2011, **1764**, 1764–1767.

45 J. D. Tice, H. Song, A. D. Lyon and R. F. Ismagilov, *Langmuir*, 2003, **19**, 9127–9133.

46 P. Garstecki, A. M. Gañán-Calvo and G. M. Whitesides, *Bull. Pol. Acad. Sci.: Tech. Sci.*, 2005, **53**, 361–372.

47 L. Shui, A. Van Den Berg and J. C. T. Eijkel, *Microfluid. Nanofluid.*, 2011, **11**, 87–92.

48 S. L. Anna and H. C. Mayer, *Phys. Fluids*, 2006, **18**, 1–13.

49 H.-H. Jeong, V. R. Yelleswarapu, S. Yadavali, D. Issadore and D. Lee, *Lab Chip*, 2015, **15**, 4387–4392.

50 V. R. Yelleswarapu, H.-H. Jeong, S. Yadavali and D. Issadore, *Lab Chip*, 2017, **17**, 1083–1094.

51 E. Amstad, M. Chemama, M. Eggersdorfer, L. R. Arriaga, M. P. Brenner and D. A. Weitz, *Lab Chip*, 2016, **16**, 4163–4172.

52 J. Kehe, A. Kulesa, A. Ortiz, C. M. Ackerman, S. G. Thakku, D. Sellers, S. Kuehn, J. Gore, J. Friedman and P. C. Blainey, *Proc. Natl. Acad. Sci. U. S. A.*, 2019, **116**, 12804–12809.

53 A. Kulesa, J. Kehe, J. E. Hurtado, P. Tawde and P. C. Blainey, *Proc. Natl. Acad. Sci. U. S. A.*, 2018, **115**, 6685–6690.

54 M. N. Hatori, S. C. Kim and A. R. Abate, *Anal. Chem.*, 2018, **90**, 9813–9820.

55 Y.-T. Kao, T. S. Kaminski, W. Postek, J. Guzowski, K. Makuch, A. Ruszczak, F. von Stetten, R. Zengerle and P. Garstecki, *Lab Chip*, 2020, **20**, 54–63.

56 C. Holtze, A. C. Rowat, J. J. Agresti, J. B. Hutchison, F. E. Angile, C. H. J. Schmitz, S. Koster, H. Duan, K. J. Humphry, R. A. Scanga, J. S. Johnson, D. Pisignano, D. A. Weitz, F. E. Angilè, C. H. J. Schmitz, S. Köster, H. Duan, K. J. Humphry, R. A. Scanga, J. S. Johnson, D. Pisignano and D. A. Weitz, *Lab Chip*, 2008, **8**, 1632–1639.

57 M. S. Chowdhury, W. Zheng, S. Kumari, J. Heyman, X. Zhang, P. Dey, D. A. Weitz and R. Haag, *Nat. Commun.*, 2019, **10**, 4546.

58 D. Liu, G. Liang, X. Lei, B. Chen, W. Wang and X. Zhou, *Anal. Chim. Acta*, 2012, **718**, 58–63.

59 A. S. Basu, *SLAS Technol.*, 2017, **22**, 369–386.

60 L. Cao, X. Cui, J. Hu, Z. Li, J. R. Choi, Q. Yang, M. Lin, L. Ying Hui and F. Xu, *Biosens. Bioelectron.*, 2017, **90**, 459–474.

61 E. Z. Macosko, A. Basu, R. Satija, J. Nemesh, K. Shekhar, M. Goldman, I. Tirosh, A. R. Bialas, N. Kamitaki, E. M. Martersteck, J. J. Trombetta, D. A. Weitz, J. R. Sanes, A. K. Shalek, A. Regev and S. A. McCarroll, *Cell*, 2015, **161**, 1202–1214.

62 A. M. Klein, L. Mazutis, I. Akartuna, N. Tallapragada, A. Veres, V. Li, L. Peshkin, D. A. Weitz and M. W. Kirschner, *Cell*, 2015, **161**, 1187–1201.

63 F. Lan, B. Demaree, N. Ahmed and A. R. Abate, *Nat. Biotechnol.*, 2017, **35**, 640–646.

64 O. Strohmeier, M. Keller, F. Schwemmer, S. Zehnle, D. Mark, F. von Stetten, R. Zengerle and N. Paust, *Chem. Soc. Rev.*, 2015, **44**, 6187–6229.

65 M. Tang, G. Wang, S.-K. Kong and H.-P. Ho, *Micromachines*, 2016, **7**, 26.

66 C. H. Chen, Y. Lu, M. L. Y. Sin, K. E. Mach, D. D. Zhang, V. Gau, J. C. Liao and P. K. Wong, *Anal. Chem.*, 2010, **82**, 1012–1019.

67 N. J. Cira, J. Y. Ho, M. E. Dueck and D. B. Weibel, *Lab Chip*, 2012, **12**, 1052–1059.

68 J. Shemesh, T. Ben Arye, J. Avesar, J. H. Kang, A. Fine, M. Super, A. Meller, D. E. Ingber and S. Levenberg, *Proc. Natl. Acad. Sci. U. S. A.*, 2014, **111**, 11293–11298.

69 J. Avesar, D. Rosenfeld, M. Truman-Rosentsvit, T. Ben-Arye, Y. Geffen, M. Bercovici and S. Levenberg, *Proc. Natl. Acad. Sci. U. S. A.*, 2017, **114**, E5787–E5795.

70 C.-W. Tsao, W. Li, S. H. Tan and N.-T. Nguyen, *Micromachines*, 2016, **7**, 225.

71 M. Azizi, M. Zaferani, B. Dogan, S. Zhang, K. W. Simpson and A. Abbaspourrad, *Anal. Chem.*, 2018, **90**, 14137–14144.

72 O. Scheler, T. S. Kaminski, A. Ruszczak and P. Garstecki, *ACS Appl. Mater. Interfaces*, 2016, **8**, 11318–11325.

73 S. J. Lin, P. H. Chao, H. W. Cheng, J. K. Wang, Y. L. Wang, Y. Y. Han and N. T. Huang, *Lab Chip*, 2022, **22**, 1805–1814.

74 M. Osaid, Y. S. Chen, C. H. Wang, A. Sinha, W. Bin Lee, P. Gopinathan, H. Bin Wu and G. Bin Lee, *Lab Chip*, 2021, **21**, 2223–2231.

75 A. S. Opalski, A. Ruszczak, Y. Promovych, M. Horka, L. Derzsi and P. Garstecki, *Micromachines*, 2020, **11**, 142.

76 W. Zeng, P. Chen, S. Li, Q. Sha, P. Li, X. Zeng, X. Feng, W. Du and B. F. Liu, *Biosens. Bioelectron.*, 2022, **205**, 114100.

77 B. Xu, Y. Du, J. Lin, M. Qi, B. Shu, X. Wen, G. Liang, B. Chen and D. Liu, *Anal. Chem.*, 2016, **88**, 11593–11600.

78 R. Mohan, C. Sanpitakseree, A. V. Desai, S. E. Sevgen, C. M. Schroeder and P. J. A. Kenis, *RSC Adv.*, 2015, **5**, 35211–35223.

79 R. Mohan, A. Mukherjee, S. E. Sevgen, C. Sanpitakseree, J. Lee, C. M. Schroeder and P. J. A. Kenis, *Biosens. Bioelectron.*, 2013, **49**, 118–125.

80 Z. Liu, H. Sun and K. Ren, *ChemPlusChem*, 2017, **82**, 792–801.

81 T. Lim, E.-G. Kim, J. Choi and S. Kwon, *Lab Chip*, 2020, **20**, 4552–4560.

82 M. Tang, X. Huang, Q. Chu, X. Ning, Y. Wang, S.-K. Kong, X. Zhang, G. Wang and H.-P. Ho, *Lab Chip*, 2018, **18**, 1452–1460.

83 J. Choi, Y. G. Jung, J. Kim, S. Kim, Y. Jung, H. Na and S. Kwon, *Lab Chip*, 2013, **13**, 280–287.

84 J. Choi, J. Yoo, M. Lee, E.-G. Kim, J. S. Lee, S. Lee, S. Joo, S. H. Song, E.-C. Kim, J. C. Lee, H. C. Kim, Y.-G. Jung and S. Kwon, *Sci. Transl. Med.*, 2014, **6**, 1–13.

85 J. Choi, H. Y. Jeong, G. Y. Lee, S. Han, S. Han, B. Jin, T. Lim, S. Kim, D. Y. Kim, H. C. Kim, E. C. Kim, S. H. Song, T. S. Kim and S. Kwon, *Sci. Rep.*, 2017, **7**, 1–13.

86 K. P. Smith and J. E. Kirby, *Antimicrob. Agents Chemother.*, 2018, **62**, 1–9.

87 Y.-G. Jung, H. Kim, S. Lee, S. Kim, E. Jo, E.-G. Kim, J. Choi, H. J. Kim, J. Yoo, H.-J. Lee, H. Kim, H. Jung, S. Ryoo and S. Kwon, *Sci. Rep.*, 2018, **8**, 8651.

88 T. Artemova, Y. Gerardin, C. Dudley, N. M. Vega and J. Gore, *Mol. Syst. Biol.*, 2015, **11**, 822.

89 C.-C. Chung, I.-F. Cheng, W.-H. Yang and H.-C. Chang, *Biomicrofluidics*, 2011, **5**, 021102.

90 C.-C. Chung, I.-F. Cheng, H.-M. Chen, H.-C. Kan, W.-H. Yang and H.-C. Chang, *Anal. Chem.*, 2012, **84**, 3347–3354.

91 I.-H. Su, W.-C. Ko, C.-H. Shih, F.-H. Yeh, Y.-N. Sun, J.-C. Chen, P.-L. Chen and H.-C. Chang, *Anal. Chem.*, 2017, **89**, 4635–4641.

92 W. Du, L. Li, K. P. Nichols and R. F. Ismagilov, *Lab Chip*, 2009, **9**, 2286–2292.

93 Q. Yi, D. Cai, M. Xiao, M. Nie, Q. Cui, J. Cheng, C. Li, J. Feng, G. Urban, Y. C. Xu, Y. Lan and W. Du, *Biosens. Bioelectron.*, 2019, **135**, 200–207.

94 J. Yoon, Y. Kim, J.-W. Suh, Y.-Y. Jin, Y.-G. Jung and W. Park, *ACS Appl. Bio Mater.*, 2020, **3**, 4798–4808.

95 V. Kara, C. Duan, K. Gupta, S. Kurosawa, D. J. Stearns-Kurosawa and K. L. Ekinci, *Lab Chip*, 2018, **18**, 743–753.

96 M. Kalashnikov, J. C. Lee, J. Campbell, A. Sharon and A. F. Sauer-Budge, *Lab Chip*, 2012, **12**, 4523–4532.

97 H. Shi, Z. Hou, Y. Zhao, K. Nie, B. Dong, L. Chao, S. Shang, M. Long and Z. Liu, *Chem. Eng. J.*, 2019, **359**, 1327–1338.

98 S. Kim, S. Lee, J.-K. Kim, H. J. Chung and J. S. Jeon, *Biomicrofluidics*, 2019, **13**, 014108.

99 N. C. Parsley, A. L. Smythers and L. M. Hicks, *Front. Cell. Infect. Microbiol.*, 2020, **10**, 503.

100 M. Kalashnikov, M. Mueller, C. McBeth, J. C. Lee, J. Campbell, A. Sharon and A. F. Sauer-Budge, *Sci. Rep.*, 2017, **7**, 1–10.

101 I. Peitz and R. Van Leeuwen, *Lab Chip*, 2010, **10**, 2944–2951.

102 P. Wang, L. Robert, J. Pelletier, W. L. Dang, F. Taddei, A. Wright and S. Jun, *Curr. Biol.*, 2010, **20**, 1099–1103.

103 L. Robert, J. Ollion, J. Robert, X. Song, I. Matic and M. Elez, *Science*, 2018, **359**, 1283–1286.

104 R. A. Bamford, A. Smith, J. Metz, G. Glover, R. W. Titball and S. Pagliara, *BMC Biol.*, 2017, **15**, 121.

105 T. Bergmiller, A. M. C. Andersson, K. Tomasek, E. Balleza, D. J. Kiviet, R. Hauschild, G. Tkačik and C. C. Guet, *Science*, 2017, **356**, 311–315.

106 N. Q. Balaban, *Science*, 2004, **305**, 1622–1625.

107 O. Goode, A. Smith, A. Zarkan, J. Cama, B. M. Invergo, D. Belgami, S. Caño-Muñiz, J. Metz, P. O'neill, A. Jeffries, I. H. Norville, J. David, D. Summers and S. Pagliara, *MBio*, 2021, **12**, 1–18.

108 U. Łapińska, M. Voliotis, K. K. Lee, A. Campey, M. R. L. Stone, B. Tuck, W. Phetsang, B. Zhang, K. Tsaneva-Atanasova, M. A. Blaskovich and S. Pagliara, *eLife*, 2022, **11**, 1–33.

109 M. Rhia, L. Stone, U. Łapin'ska, Ł. Łapin'ska, S. Pagliara, M. Masi, J. T. Blanchfield, M. A. Cooper and M. A. T. Blaskovich, *RSC Chem. Biol.*, 2020, **1**, 395–404.

110 I. E. Kepiro, I. Marzuoli, K. Hammond, X. Ba, H. Lewis, M. Shaw, S. B. Gunnoo, E. De Santis, U. Łapińska, S. Pagliara, M. A. Holmes, C. D. Lorenz, B. W. Hoogenboom, F. Fraternali and M. G. Ryadnov, *ACS Nano*, 2020, **14**, 1609–1622.

111 E. L. Attrill, R. Claydon, U. Łapińska, M. Recker, S. Meaden, A. T. Brown, E. R. Westra, S. V. Harding and S. Pagliara, *PLoS Biol.*, 2021, **19**, e3001406.

112 Y. Lu, J. Gao, D. D. Zhang, V. Gau, J. C. Liao and P. K. Wong, *Anal. Chem.*, 2013, **85**, 3971–3976.

113 Ö. Baltekin, A. Boucharin, E. Tano, D. I. Andersson and J. Elf, *Proc. Natl. Acad. Sci. U. S. A.*, 2017, **114**, 9170–9175.

114 H. Li, P. Torab, K. E. Mach, C. Surrette, M. R. England, D. W. Craft, N. J. Thomas, J. C. Liao, C. Puleo and P. K. Wong, *Proc. Natl. Acad. Sci. U. S. A.*, 2019, **116**, 10270–10279.

115 B. Li, Y. Qiu, A. Glidle, D. McIlvenna, Q. Luo, J. Cooper, H. C. Shi and H. Yin, *Anal. Chem.*, 2014, **86**, 3131–3137.

116 Y. Yang, K. Gupta and K. L. Ekinci, *Proc. Natl. Acad. Sci. U. S. A.*, 2020, **117**, 10639–10644.

117 A. A. Sklavounos, C. R. Nemr, S. O. Kelley and A. R. Wheeler, *Lab Chip*, 2021, **21**, 4208–4222.

118 I. Sinn, P. Kinnunen, T. Albertson, B. H. McNaughton, D. W. Newton, M. A. Burns and R. Kopelman, *Lab Chip*, 2011, **11**, 2604–2611.

119 G. Amselem, C. Guermonprez, B. Drogue, S. Michelin and C. N. Baroud, *Lab Chip*, 2016, **16**, 4200–4211.

120 A. Saint-Sardos, S. Sart, K. Lippera, E. Brient-Litzler, S. Michelin, G. Amselem and C. N. Baroud, *Small*, 2020, **16**, 2002303.

121 P. Sabhachandani, S. Sarkar, P. C. Zucchi, B. A. Whitfield, J. E. Kirby, E. B. Hirsch and T. Konry, *Microchim. Acta*, 2017, **184**, 4619–4628.

122 W. Kang, S. Sarkar, Z. S. Lin, S. McKenney and T. Konry, *Anal. Chem.*, 2019, **91**, 6242–6249.

123 Z. Liu, C. Duan, S. Jiang, C. Zhu, Y. Ma and T. Fu, *J. Ind. Eng. Chem.*, 2020, **92**, 18–40.

124 L. Derzsi, T. S. Kaminski and P. Garstecki, *Lab Chip*, 2016, **16**, 893–901.

125 E. Brouzes, M. Medkova, N. Savenelli, D. Marran, M. Twardowski, J. B. Hutchison, J. M. Rothberg, D. R. Link, N. Perrimon and M. L. Samuels, *Proc. Natl. Acad. Sci. U. S. A.*, 2009, **106**, 14195–14200.

126 S. Jakiela, T. S. Kaminski, O. Cybulski, D. B. Weibel and P. Garstecki, *Angew. Chem., Int. Ed.*, 2013, **52**, 8908–8911.

127 L. Baraban, F. Bertholle, M. L. M. Salverda, N. Bremond, P. Panizza, J. Baudry, J. A. G. M. De Visser and J. Bibette, *Lab Chip*, 2011, **11**, 4057–4062.

128 S. Jakiela, T. S. Kaminski, O. Cybulski, D. B. Weibel and P. Garstecki, *Angew. Chem.*, 2013, **125**, 9076–9079.

129 J. Q. Boedicker, L. Li, T. R. Kline and R. F. Ismagilov, *Lab Chip*, 2008, **8**, 1265–1272.

130 W. Postek, P. Gargulinski, O. Scheler, T. S. Kaminski and P. Garstecki, *Lab Chip*, 2018, **18**, 3668–3677.

131 H. Li, P. Zhang, K. Hsieh and T.-H. Wang, *Lab Chip*, 2022, **22**, 621–631.

132 X. Liu, R. E. Painter, K. Enesa, D. Holmes, G. Whyte, C. G. Garlisi, F. J. Monsma, M. Rehak, F. F. Craig and C. A. Smith, *Lab Chip*, 2016, **16**, 1636–1643.

133 F. Lyu, M. Pan, S. Patil, J.-H. Wang, A. C. Matin, J. R. Andrews and S. K. Y. Tang, *Sens. Actuators, B*, 2018, **270**, 396–404.

134 O. Scheler, K. Makuch, P. R. Debski, M. Horka, A. Ruszczak, N. Pacocha, K. Sozański, O.-P. Smolander, W. Postek and P. Garstecki, *Sci. Rep.*, 2020, **10**, 3282.

135 A. M. Kaushik, K. Hsieh, L. Chen, D. J. Shin, J. C. Liao and T. H. Wang, *Biosens. Bioelectron.*, 2017, **97**, 260–266.

136 A. R. Abate, T. Hung, P. Mary, J. J. Agresti and D. A. Weitz, *Proc. Natl. Acad. Sci. U. S. A.*, 2010, **107**, 19163–19166.

137 A. Funfak, R. Hartung, J. Cao, K. Martin, K.-H. Wiesmüller, O. S. Wolfbeis and J. M. Köhler, *Sens. Actuators, B*, 2009, **142**, 66–72.

138 K. Churski, T. S. Kaminski, S. Jakiela, W. Kamysz, W. Baranska-Rybak, D. B. Weibel and P. Garstecki, *Lab Chip*, 2012, **12**, 1629–1637.

139 L. Jiang, L. Boitard, P. Broyer, A. C. Chareire, P. Bourne-Branchu, P. Mahé, M. Tournoud, C. Franceschi, G. Zambardi, J. Baudry and J. Bibette, *Eur. J. Clin. Microbiol. Infect. Dis.*, 2016, **35**, 415–422.

140 European Committee for Antimicrobial Susceptibility Testing (EUCAST) of the European Society of Clinical Microbiology and Infectious Diseases (ESCMID), Determination of minimum inhibitory concentrations (MICs) ofantibacterial agents by broth dilution, *Clin. Microbiol. Infect.*, 2003, **9**, ix–xv.

141 Clinical and Laboratory Standards Institute, CLSI Doc. M100-S16CLSI, Wayne, PA.

142 K. Lewis, *Annu. Rev. Microbiol.*, 2010, **64**, 357–372.

143 W. Hong, C. W. Karanja, N. S. Abutaleb, W. Younis, X. Zhang, M. N. Seleem and J.-X. Cheng, *Anal. Chem.*, 2018, **90**, 3737–3743.

144 Y. Liu, T. Lehnert and M. A. M. Gijs, *Lab Chip*, 2020, **20**, 3144–3157.

145 P. Jusková, S. Schmitt, A. Kling, D. G. Rackus, M. Held, A. Egli and P. S. Dittrich, *ACS Sens.*, 2021, **6**, 2202–2210.

146 F. Courtois, L. F. Olguin, G. Whyte, A. B. Theberge, W. T. S. Huck, F. Hollfelder and C. Abell, *Anal. Chem.*, 2009, **81**, 3008–3016.

147 Y. Chen, A. Wijaya Gani and S. K. Y. Tang, *Lab Chip*, 2012, **12**, 5093–5103.

148 T. S. Kaminski, O. Scheler and P. Garstecki, *Lab Chip*, 2016, **16**, 2168–2187.

149 P. Gruner, B. Riechers, B. Semin, J. Lim, A. Johnston, K. Short and J.-C. Baret, *Nat. Commun.*, 2016, **7**, 10392.

150 N. Pacocha, J. Bogusławski, M. Horka, K. Makuch, K. Liżewski, M. Wojtkowski and P. Garstecki, *Anal. Chem.*, 2021, **93**, 843–850.

151 I. P. Alves and N. M. Reis, *Biosens. Bioelectron.*, 2019, **145**, 111624.

152 X. Cui, L. Ren, Y. Shan, X. Wang, Z. Yang, C. Li, J. Xu and B. Ma, *Analyst*, 2018, **143**, 3309–3316.

153 E. Um, E. Rha, S.-L. Choi, S.-G. Lee and J.-K. Park, *Lab Chip*, 2012, **12**, 1594.

154 P. Sharma, P. Pratim Pandey, S. Jain, X. Liu, H. Li, M. Zhan, P. Greulich, J. Doležal, D. Taylor, N. Verdon, P. Lomax, R. J. Allen and S. Titmuss, *Phys. Biol.*, 2022, **19**, 026003.

155 S. Hengoju, S. Wohlfeil, A. S. Munser, S. Boehme, E. Beckert, O. Shvydkiv, M. Tovar, M. Roth and M. A. Rosenbaum, *Biomicrofluidics*, 2020, **14**, 024109.

156 M. Horka, S. Sun, A. Ruszczak, P. Garstecki and T. Mayr, *Anal. Chem.*, 2016, **88**, 12006–12012.

157 L. Boitard, D. Cottinet, C. Kleinschmitt, N. Bremond, J. Baudry, G. Yvert and J. Bibette, *Proc. Natl. Acad. Sci. U. S. A.*, 2012, **109**, 7181–7186.

158 E. Zang, S. Brandes, M. Tovar, K. Martin, F. Mech, P. Horbert, T. Henkel, M. T. Figge and M. Roth, *Lab Chip*, 2013, **13**, 3707–3713.

159 A. C. Hatch, J. S. Fisher, A. R. Tovar, A. T. Hsieh, R. Lin, S. L. Pentoney, D. L. Yang and A. P. Lee, *Lab Chip*, 2011, **11**, 3838.

160 B. J. Hindson, K. D. Ness, D. A. Masquelier, P. Belgrader, N. J. Heredia, A. J. Makarewicz, I. J. Bright, M. Y. Lucero, A. L. Hiddessen, T. C. Legler, T. K. Kitano, M. R. Hodel, J. F. Petersen, P. W. Wyatt, E. R. Steenblock, P. H. Shah, L. J. Bousse, C. B. Troup, J. C. Mellen, D. K. Wittmann, N. G. Erndt, T. H. Cauley, R. T. Koehler, A. P. So, S. Dube, K. A. Rose, L. Montesclaros, S. Wang, D. P. Stumbo, S. P. Hodges, S. Romine, F. P. Milanovich, H. E. White, J. F. Regan, G. A. Karlin-Neumann, C. M. Hindson, S. Saxonov and B. W. Colston, *Anal. Chem.*, 2011, **83**, 8604–8610.

161 T. J. Abram, H. Cherukury, C. Y. Ou, T. Vu, M. Toledano, Y. Li, J. T. Grunwald, M. N. Toosky, D. F. Tifrea, A. Slepenkin, J. Chong, L. Kong, D. V. Del Pozo, K. T. La, L. Labanieh, J. Zimak, B. Shen, S. S. Huang, E. Gratton, E. M. Peterson and W. Zhao, *Lab Chip*, 2020, **20**, 477–489.

162 J. D. Bard and F. Lee, *Clin. Microbiol. Newsl.*, 2018, **40**, 87–95.

163 F. C. Tenover, *Clin. Lab. Med.*, 1989, **9**, 341–347.

164 P. Athamanolap, K. Hsieh, C. M. O'Keefe, Y. Zhang, S. Yang and T.-H. Wang, *Anal. Chem.*, 2019, **91**, 12784–12792.

165 H. W. Hou, R. P. Bhattacharyya, D. T. Hung and J. Han, *Lab Chip*, 2015, **15**, 2297–2307.

166 N. G. Schoepp, E. M. Khorosheva, T. S. Schlappi, M. S. Curtis, R. M. Humphries, J. A. Hindler and R. F. Ismagilov, *Angew. Chem., Int. Ed.*, 2016, **55**, 9557–9561.

167 N. G. Schoepp, T. S. Schlappi, M. S. Curtis, S. S. Butkovich, S. Miller, R. M. Humphries and R. F. Ismagilov, *Sci. Transl. Med.*, 2017, **9**, eaal3693.

168 T. Notomi, H. Okayama, H. Masubuchi, T. Yonekawa, K. Watanabe, N. Amino and T. Hase, *Nucleic Acids Res.*, 2000, **28**, 63e.

169 T. Khazaei, J. T. Barlow, N. G. Schoepp and R. F. Ismagilov, *Sci. Rep.*, 2018, **8**, 11606.

170 A. M. Kaushik, K. Hsieh, K. E. Mach, S. Lewis, C. M. Puleo, K. C. Carroll, J. C. Liao and T. Wang, *Adv. Sci.*, 2021, 2003419.

171 G. Longo, L. Alonso-Sarduy, L. Marques Rio, A. Bizzini, A. Trampuz, J. Notz, G. Dietler and S. Kasas, *Nat. Nanotechnol.*, 2013, **8**(7), 522–526.

172 N. Cermak, S. Olcum, F. F. Delgado, S. C. Wasserman, K. R. Payer, M. A. Murakami, S. M. Knudsen, R. J. Kimmerling, M. M. Stevens, Y. Kikuchi, A. Sandikci, M. Ogawa, V. Agache, F. Baléras, D. M. Weinstock and S. R. Manalis, *Nat. Biotechnol.*, 2016, **34**, 1052–1059.

173 H. Etayash, M. F. Khan, K. Kaur and T. Thundat, *Nat. Commun.*, 2016, **7**, 12947.

174 I. Bennett, A. L. B. Pyne and R. A. McKendry, *ACS Sens.*, 2020, **5**, 3133–3139.

175 M. Godin, F. F. Delgado, S. Son, W. H. Grover, A. K. Bryan, A. Tzur, P. Jorgensen, K. Payer, A. D. Grossman, M. W. Kirschner and S. R. Manalis, *Nat. Methods*, 2010, **7**(5), 387–390.

176 P. Stupar, O. Opota, G. Longo, G. Prod'hom, G. Dietler, G. Greub and S. Kasas, *Clin. Microbiol. Infect.*, 2017, **23**, 400–405.

177 F. Pujol-Vila, R. Villa and M. Alvarez, *Front. Mech. Eng.*, 2020, **6**, 44.

178 P. Cady, S. W. Dufour, J. Shaw and S. J. Kraeger, *J. Clin. Microbiol.*, 1978, **7**, 265–272.

179 M. S. Mannoor, S. Zhang, A. J. Link and M. C. McAlpine, *Proc. Natl. Acad. Sci. U. S. A.*, 2010, **107**, 19207–19212.

180 D. C. Spencer, T. F. Paton, K. T. Mulroney, T. J. J. Inglis, J. M. Sutton and H. Morgan, *Nat. Commun.*, 2020, **11**, 5328.

181 C. Honrado, P. Bisegna, N. S. Swami and F. Caselli, *Lab Chip*, 2021, **21**, 22–54.

182 M. J. Kellner, J. G. Koob, J. S. Gootenberg, O. O. Abudayyeh and F. Zhang, *Nat. Protoc.*, 2019, **14**, 2986–3012.

183 C. M. Ackerman, C. Myhrvold, S. G. Thakku, C. A. Freije, H. C. Metsky, D. K. Yang, S. H. Ye, C. K. Boehm, T.-S. F. Kosoko-Thoroddsen, J. Kehe, T. G. Nguyen, A. Carter, A. Kulesa, J. R. Barnes, V. G. Dugan, D. T. Hung, P. C. Blainey and P. C. Sabeti, *Nature*, 2020, **582**, 277–282.

184 S. G. Thakku, C. M. Ackerman, C. Myhrvold, R. P. Bhattacharyya, J. Livny, P. Ma, G. I. Gomez, P. C. Sabeti, P. C. Blainey and D. T. Hung, *PNAS Nexus*, 2022, **1**, 1–10.

185 X. Wang, Z. Liu and Y. Pang, *RSC Adv.*, 2017, **7**, 29966–29984.

186 N. L. Jeon, S. K. W. Dertinger, D. T. Chiu, I. S. Choi, A. D. Stroock and G. Whitesides, *Langmuir*, 2000, **16**, 8311–8316.

187 O. Miller, A. Harrak, T. Mangeat, J.-C. Baret, L. Frenz, B. Debs, E. Mayot, M. Samuels, E. Rooney, P. Dieu, M. Galvan and A. Griffiths, *Proc. Natl. Acad. Sci. U. S. A.*, 2012, **109**, 378–383.

188 X. Niu, F. Gielen, J. B. Edel and A. J. deMello, *Nat. Chem.*, 2011, **3**, 437–442.

189 W. Postek, T. S. Kaminski and P. Garstecki, *Analyst*, 2017, **142**, 2901–2911.

190 M. Sun, S. S. Bithi and S. A. Vanapalli, *Lab Chip*, 2012, **11**, 3949–3952.

191 M. Sun and S. A. Vanapalli, *Anal. Chem.*, 2013, **85**, 2044–2048.

192 K. I. Udekwu, N. Parrish, P. Ankomah, F. Baquero and B. R. Levin, *J. Antimicrob. Chemother.*, 2009, **63**, 745–757.

193 C. Tan, R. P. Smith, J. K. Srimani, K. A. Riccione, S. Prasada, M. Kuehn and L. You, *Mol. Syst. Biol.*, 2012, **8**, 617.

194 W. A. Craig, S. M. Bhavnani and P. G. Ambrose, *Diagn. Microbiol. Infect. Dis.*, 2004, **50**, 229–230.

195 Clinical and Laboratory Standards Institute, CLSI Doc. M07-A10, Clin. Lab. Stand. Institute, Wayne, PA.

196 J. Q. Boedicker, M. E. Vincent and R. F. Ismagilov, *Angew. Chem., Int. Ed.*, 2009, **48**, 5908–5911.

197 D. I. Andersson, H. Nicoloff and K. Hjort, *Nat. Rev. Microbiol.*, 2019, **17**(8), 479–496.

198 S. S. Y. Wong, P. L. Ho, P. C. Y. Woo and K. Y. Yuen, *Clin. Infect. Dis.*, 1999, **29**, 760–767.

199 W. Yau, R. J. Owen, A. Poudyal, J. M. Bell, J. D. Turnidge, H. H. Yu, R. L. Nation and J. Li, *J. Infect.*, 2009, **58**, 138–144.

200 H. Nicoloff, K. Hjort, B. R. Levin and D. I. Andersson, *Nat. Microbiol.*, 2019, **4**, 504–514.

201 D. M. Hermes, C. Pormann Pitt, L. Lutz, A. B. Teixeira, V. B. Ribeiro, B. Netto, A. F. Martins, A. P. Zavascki and A. L. Barth, *J. Med. Microbiol.*, 2013, **62**, 1184–1189.

202 J. D. Sun, S. F. Huang, S. S. Yang, S. L. Pu, C. M. Zhang and L. P. Zhang, *Clin. Microbiol. Infect.*, 2015, **21**(5), 469.

203 A. E. B. da Silva, A. F. Martins, C. S. Nodari, C. M. Magagnin and A. L. Barth, *Eur. J. Clin. Microbiol. Infect. Dis.*, 2017, **37**(1), 185–186.

204 T. Pelaez, E. Cercenado, L. Alcala, M. Marin, A. Martin-Lopez, J. Martinez-Alarcon, P. Catalan, M. Sanchez-Somolinos and E. Bouza, *J. Clin. Microbiol.*, 2008, **46**, 3028–3032.

205 O. M. El-Halfawy and M. A. Valvano, *Clin. Microbiol. Rev.*, 2015, **28**, 191–207.

206 L. Sun, S. Talarico, L. Yao, L. He, S. Self, Y. You, H. Zhang, Y. Zhang, Y. Guo, G. Liu, N. R. Salama and J. Zhang, *J. Clin. Microbiol.*, 2018, **6**(9), DOI: 10.1128/JCM.00019-18.

207 A. Raj and A. van Oudenaarden, *Cell*, 2008, **135**, 216–226.

208 A. Brauner, O. Fridman, O. Gefen and N. Q. Balaban, *Nat. Rev. Microbiol.*, 2016, **14**, 320–330.

209 N. Balaban, *Curr. Opin. Genet. Dev.*, 2011, **21**, 768–775.

210 B. P. Conlon, S. E. Rowe, A. B. Gandt, A. S. Nuxoll, N. P. Donegan, E. A. Zalis, G. Clair, J. N. Adkins, A. L. Cheung and K. Lewis, *Nat. Microbiol.*, 2016, **1**, 16051.

211 E. A. Zalis, A. S. Nuxoll, S. Manuse, G. Clair, L. C. Radlinski and B. P. Conlon, J. Adkins and K. Lewis, *MBio*, 2019, **10**(5), e-01930-19.

212 L. Tuchscherr, M. Bischoff, S. M. Lattar, M. Noto Llana, H. Pförtner, S. Niemann, J. Geraci, H. Van de Vyver, M. J. Fraunholz, A. L. Cheung, M. Herrmann, U. Völker, D. O. Sordelli, G. Peters and B. Löffler, *PLoS Pathog.*, 2015, **11**(4), e1004870.

213 P. Debski, K. Sklodowska, J. Michalski, P. Korczyk, M. Dolata and S. Jakiela, *Micromachines*, 2018, **9**, 469.

214 M. Abolhasani and K. F. Jensen, *Lab Chip*, 2016, **16**, 2775–2784.

215 D. Cottinet, F. Condamine, N. Bremond, A. D. Griffiths, P. B. Rainey, J. A. G. M. de Visser, J. Baudry and J. Bibette, *PLoS One*, 2016, **11**, e0152395.

216 M. Pousti, M. P. Zarabadi, M. Abbaszadeh Amirdehi, F. Paquet-Mercier and J. Greener, *Analyst*, 2019, **144**, 68–86.

217 C. B. Chang, J. N. Wilking, S.-H. Kim, H. C. Shum and D. A. Weitz, *Small*, 2015, **11**, 3954–3961.

218 MarketsandMarkets, Antimicrobial Susceptibility Testing Market by Product (Manual, Automated Susceptibility Testing System), Type (Antibacterial, Antifungal), Application (Clinical Diagnostics), Method (ETEST, Disk Diffusion), End-User - Global Forecasts to 2025, 2020.